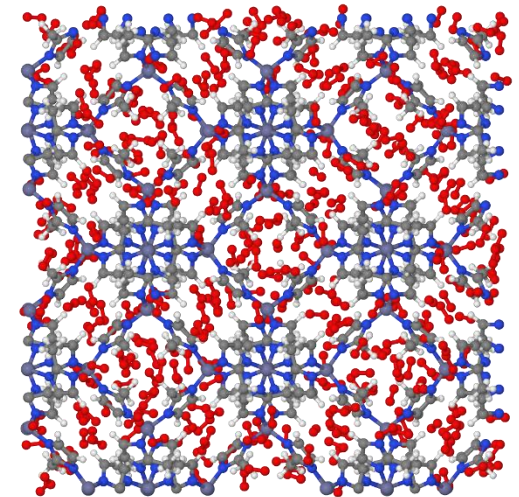
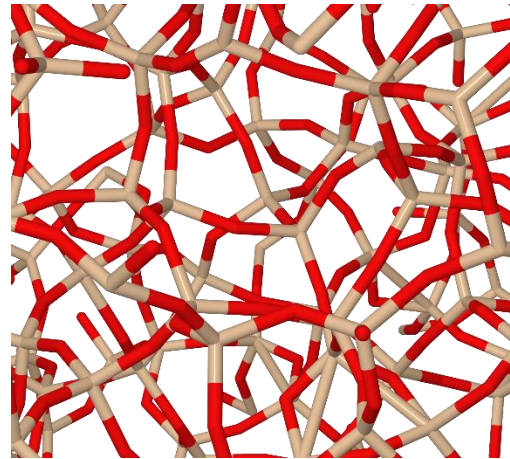
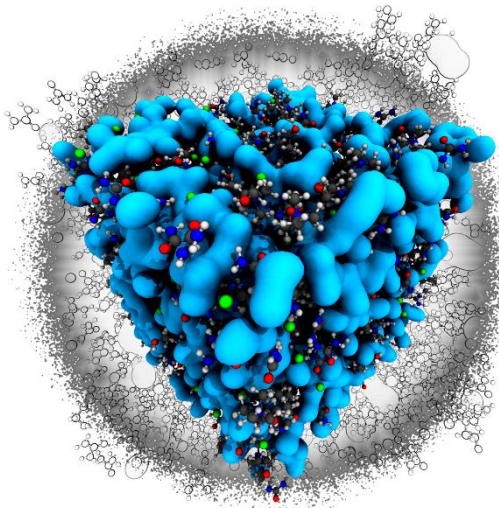


Empirical Potential Structure Refinement (EPSR): A method for structural modelling of liquids, glasses and complex nanoscale systems

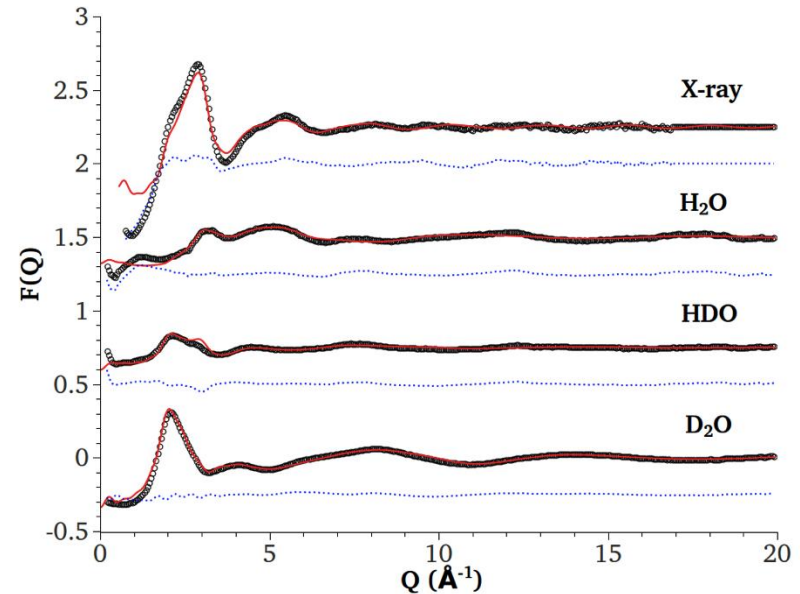
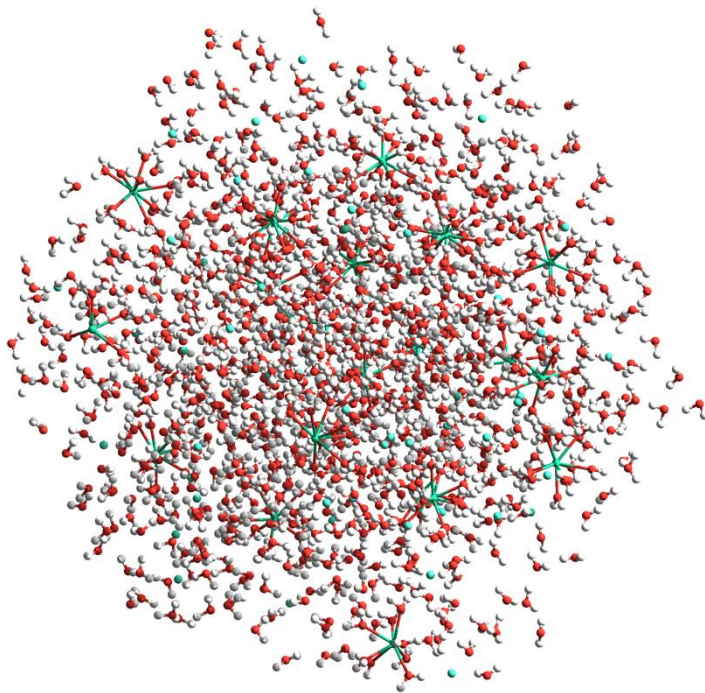
D.T.Bowron¹ and T. G. A. Youngs¹

¹ ISIS Neutron and Muon Facility, UKRI Science and Technology Facilities Council,
Rutherford Appleton Laboratory, Chilton, Didcot, OX11 0QX, UK



Empirical Potential Structure Refinement

A computational method developed by **Dr Alan Soper FRS**, for building atomic and molecular models of structurally disordered systems, that are consistent with neutron and x-ray scattering data, and known physical/chemical constraints.



- [1] A. K. Soper, *Chem. Phys.* **202**, 295-306 (1996)
- [2] A. K. Soper, *Physical Review B*, **72**, 104204 (2005)
- [3] A. K. Soper *J. Phys. Condens. Matt.* **19**, 335206 (2007)

EPSR ≠ Computer simulation

Computer “simulations allow us to develop and test models, to evaluate approximate theories of liquids, and to obtain detailed information about the structure and dynamics of *model* liquids at the molecular level.” *Computer Simulation of Liquids*, M.P.Allen and D.J.Tildesley (Clarendon Press, Oxford 1987)

EPSR allows us to build atomistic models of *real* liquids (and glasses and complex nanoscale systems) that have been characterized by neutron or X-ray scattering methods, and to test the consequences of our underlying assumptions via refinement against experimental observables.

EPSR is built on a Monte Carlo simulation engine

Its ingredients are:

(1) A computer representation of a box of atoms and molecules – essentially a store of coordinates.

(2) A set of potential energy functions to model the interactions between the atoms and molecules in the box.

(3) A set of rules by which the atoms, molecules, functional groups within the model are moved e.g.

- (a) Atomic translations
- (b) Molecule translations
- (c) Molecule rotations
- (d) Molecule functional group rotations
- (e) Torsional operations on molecules etc.

(4) A set of tools to interrogate the development of the interatomic and intermolecular structures that the model will produce.

EPSR method

Classical

Molecular mechanics
(Empirical force fields)

and

Experimental Data

Neutron Diffraction
(Nuclear correlations)

X-ray Diffraction
(Electron density
correlations)

EXAFS Spectroscopy
(Chemically specific
electron density)

Atomic Interaction Potentials

Atomistic modeling engine

Metropolis Monte Carlo

=> Value of the resulting model is limited
by the information content of the
experimental data

The total potential runs and EPSR refinement

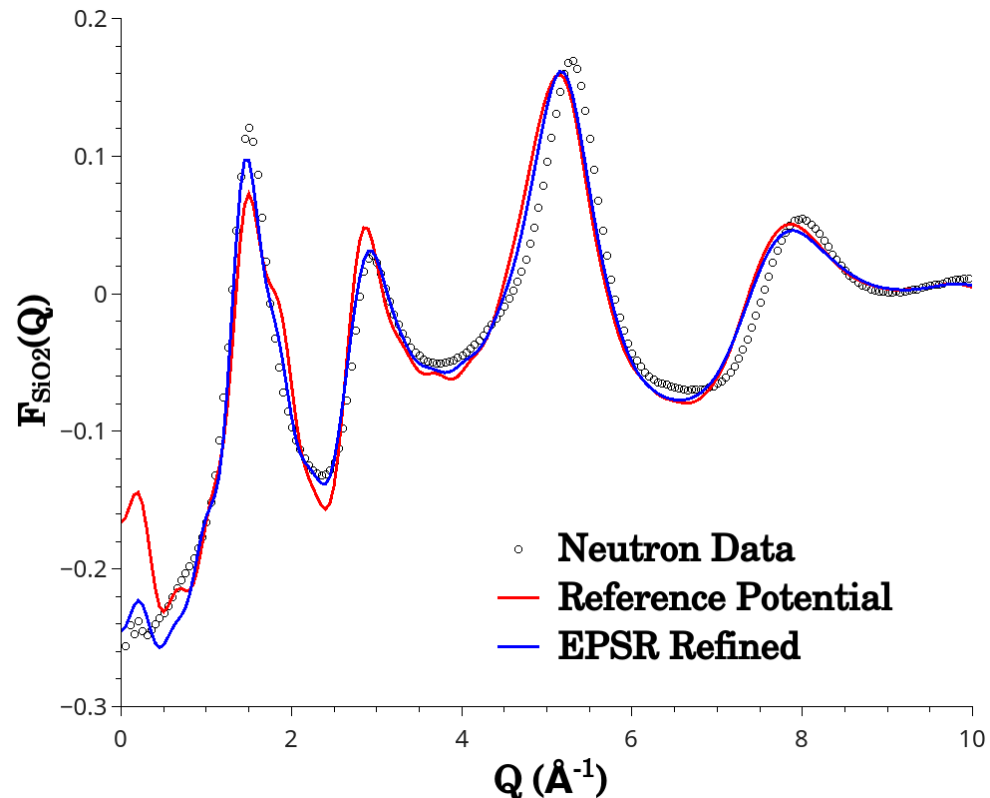
$$U_{\alpha\beta} = U_{\alpha\beta}^{ref}(r) + U_{\alpha\beta}^{EP}(r)$$

$$U^{ref} = \frac{1}{2} \sum_{i, j \neq i} \sum_{\alpha, \beta} \left(4 \epsilon_{\alpha\beta} \left[\left(\frac{\sigma_{\alpha\beta}}{r_{\alpha_i} \beta_j} \right)^n - \left(\frac{\sigma_{\alpha\beta}}{r_{\alpha_i} \beta_j} \right)^6 \right] + \frac{q_{\alpha} q_{\beta}}{4 \pi \epsilon_0 r_{\alpha_i \beta_j}} \right)$$

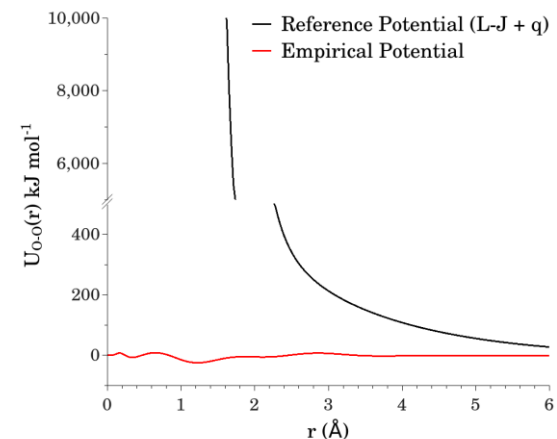
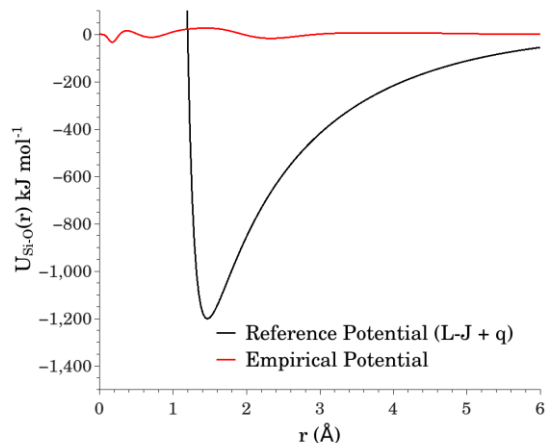
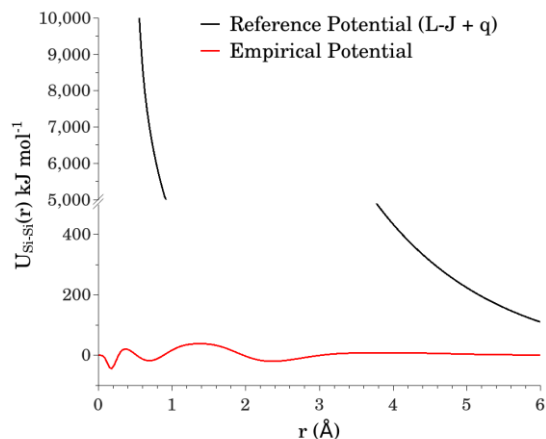
$$U^{tot} = \frac{1}{2} \sum_{i, j \neq i} \sum_{\alpha, \beta} \left(4 \epsilon_{\alpha\beta} \left[\left(\frac{\sigma_{\alpha\beta}}{r_{\alpha_i} \beta_j} \right)^n - \left(\frac{\sigma_{\alpha\beta}}{r_{\alpha_i} \beta_j} \right)^6 \right] + \frac{q_{\alpha} q_{\beta}}{4 \pi \epsilon_0 r_{\alpha_i \beta_j}} + U_{\alpha\beta}^{EP}(r) \right)$$

The result of performing an EPSR refinement

Refining a reference potential model against scattering data drives the calculated structure factor of the model towards improved agreement with the experimentally measured function.



The total potential runs and EPSR refinement



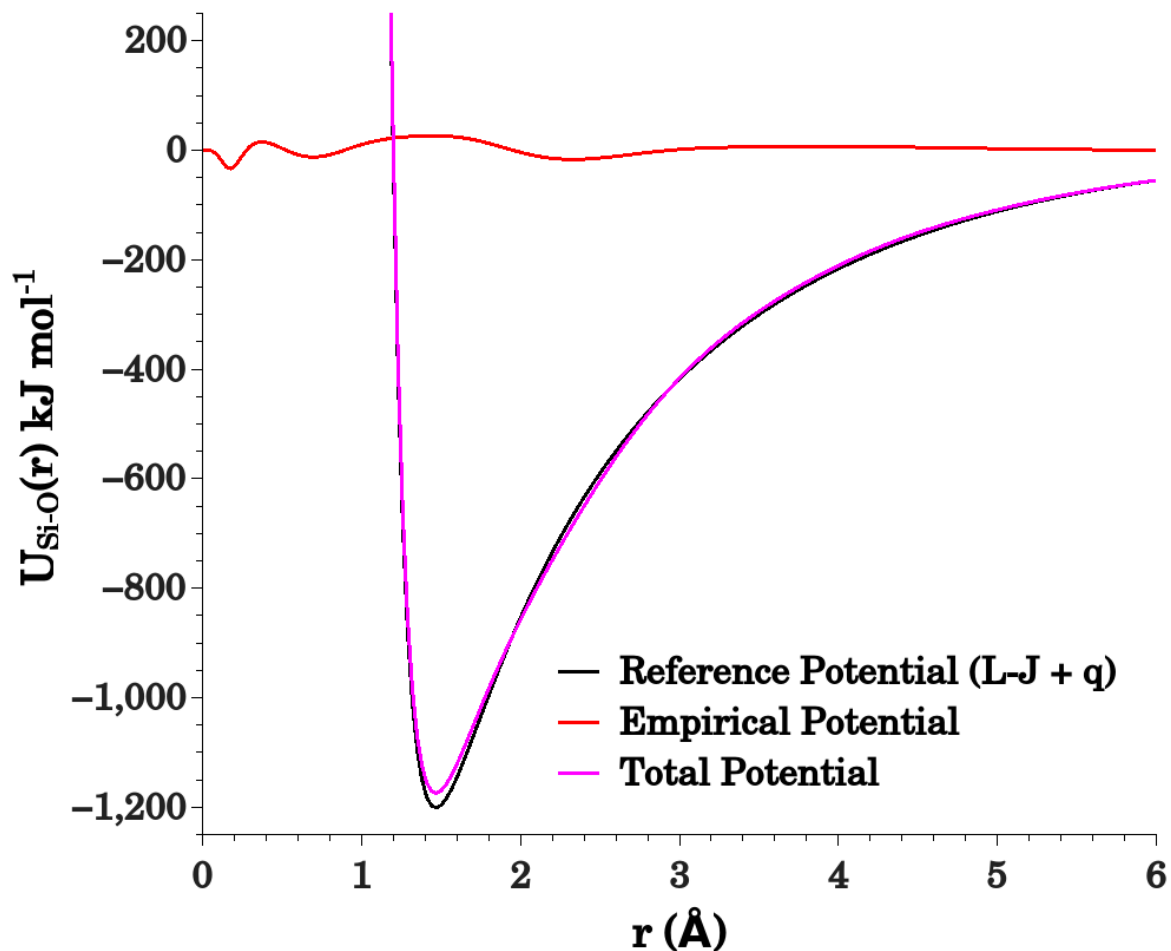
$$U_{\alpha\beta} = U_{\alpha\beta}^{ref}(r) + U_{\alpha\beta}^{EP}(r)$$

Element	σ (Å)	ϵ (kJmol ⁻¹)	q (e)
Si	1.03	0.1750	+2
O	3.60	0.1625	-1

$$U^{ref} = \frac{1}{2} \sum_{i,j \neq i} \sum_{\alpha,\beta} \left(4\epsilon_{\alpha\beta} \left[\left(\frac{\sigma_{\alpha\beta}}{r_{\alpha_i}\beta_j} \right)^n - \left(\frac{\sigma_{\alpha\beta}}{r_{\alpha_i}\beta_j} \right)^6 \right] + \frac{q_{\alpha}q_{\beta}}{4\pi\epsilon_0 r_{\alpha_i}\beta_j} \right)$$

$$U^{tot} = \frac{1}{2} \sum_{i,j \neq i} \sum_{\alpha,\beta} \left(4\epsilon_{\alpha\beta} \left[\left(\frac{\sigma_{\alpha\beta}}{r_{\alpha_i}\beta_j} \right)^n - \left(\frac{\sigma_{\alpha\beta}}{r_{\alpha_i}\beta_j} \right)^6 \right] + \frac{q_{\alpha}q_{\beta}}{4\pi\epsilon_0 r_{\alpha_i}\beta_j} + U_{\alpha\beta}^{EP}(r) \right)$$

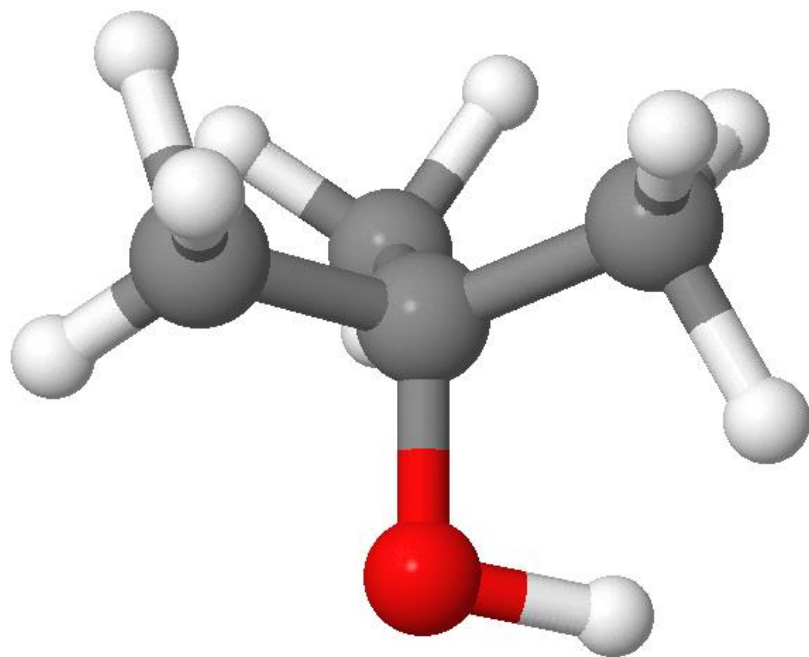
The total potential runs and EPSR refinement



$$U_{\alpha\beta} = U_{\alpha\beta}^{ref}(r) + U_{\alpha\beta}^{EP}(r)$$

EPSR is designed to function with both atoms and molecules

Molecules are defined using distance constraints



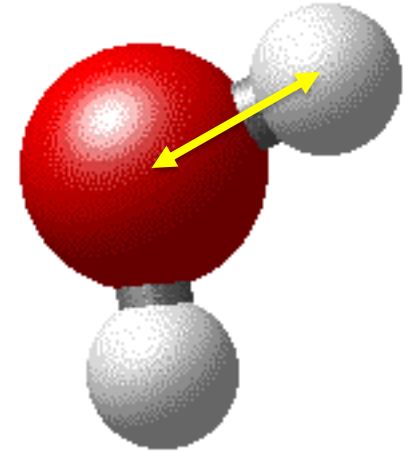
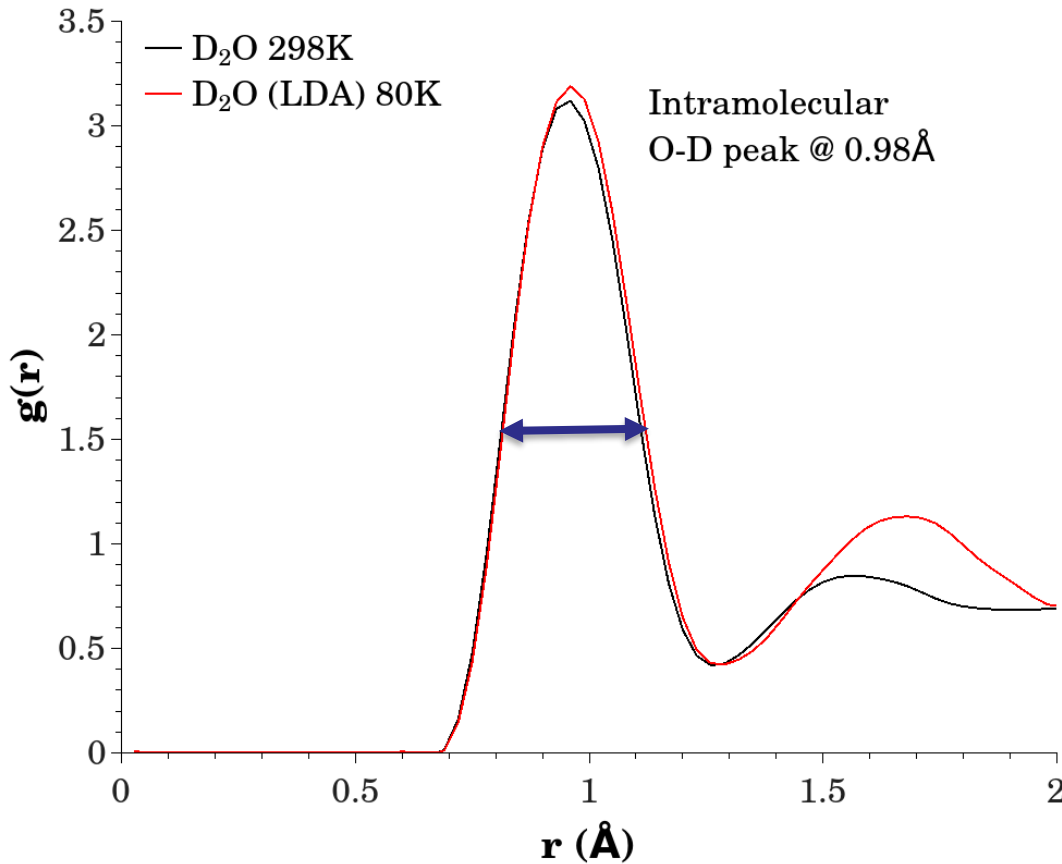
Jmol

Within EPSR, molecules are defined by a criterion for the distances between first and second neighbour atoms. These two distances effectively constrain the angles.

For simplicity, the builder programs also allow you to specify the molecular structure in terms of first neighbour distances and angles.

Molecules are flexible to account for observed disorder

(and consequently every molecule in the model is slightly different)



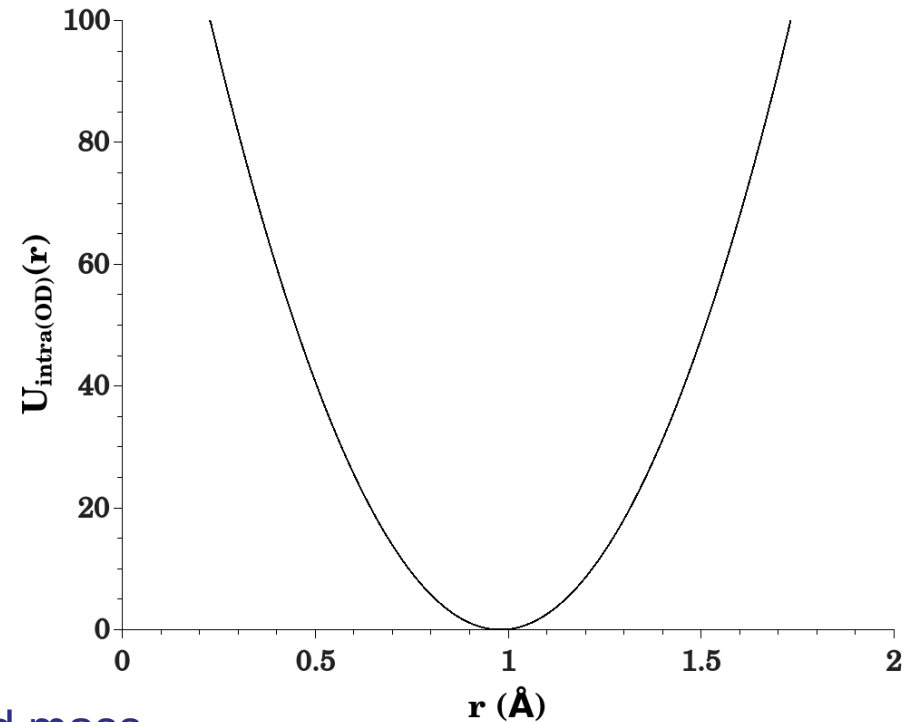
Molecules are flexible to account for observed disorder

$$U_{intra} = C \sum_i \sum_{\alpha\beta \neq \alpha} \frac{(r_{\alpha_i\beta_i} - d_{\alpha\beta})^2}{2w_{\alpha\beta}^2}$$

$$C = 130 \text{ \AA}^{-1} \text{ amu}^{-1}$$

$$d_{\alpha\beta} = 0.98 \text{ \AA}$$

$$w^2 = 0.98 / ((16 \times 2) / (16 + 2))^{1/2}$$



Average distance

$$w_{\alpha\beta}^2 = \frac{d_{\alpha\beta}}{(\mu_{\alpha\beta})^{1/2}}$$

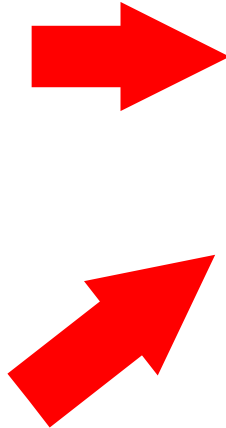
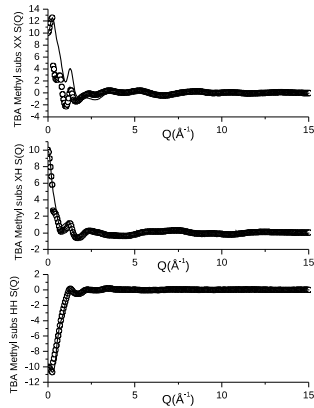
Reduced mass

$$\mu_{\alpha\beta} = \frac{M_{\alpha} M_{\beta}}{(M_{\alpha} + M_{\beta})}$$

Broadening function to avoid individual Debye-Waller factors for each distance

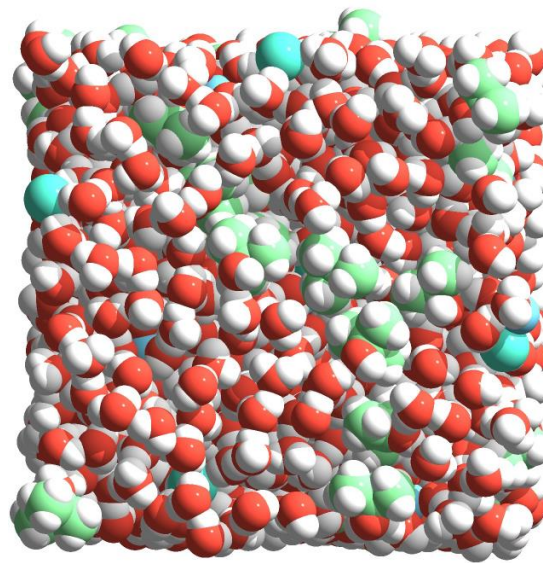
INPUT

Experimental data



Constraints such as:
Density
Molecular geometry

EPSR



$$U_{\alpha\beta}^N = U_{\alpha\beta}^O(r) + U_{\alpha\beta}^{\Delta EP}(r)$$

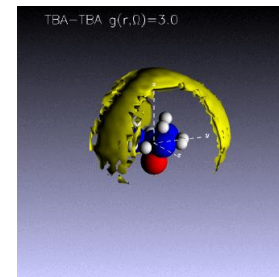
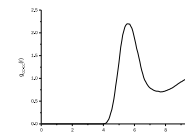
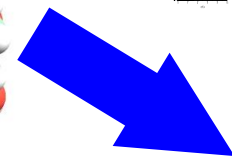
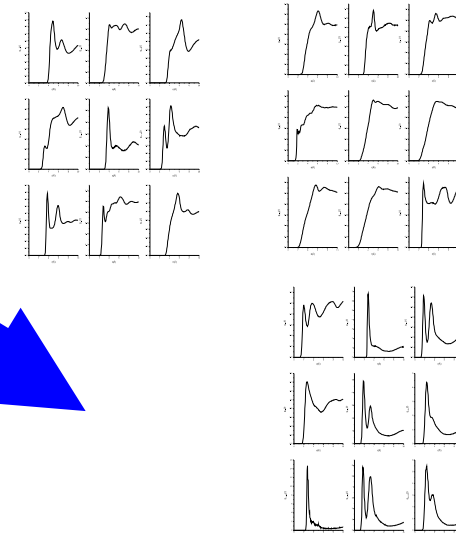
$$U_{\alpha\beta}^O(r) \approx U_{\alpha\beta}^N(r)$$

$$S_{\alpha\beta}^{Model}(Q) \approx S_{\alpha\beta}^{Data}(Q)$$

$$g_{\alpha\beta}^{Model}(r) \approx g_{\alpha\beta}^{Data}(r)$$

OUTPUT

A wealth of structural information



EPSR: a summary

Understanding the limits of what can safely concluded from disordered materials diffraction data

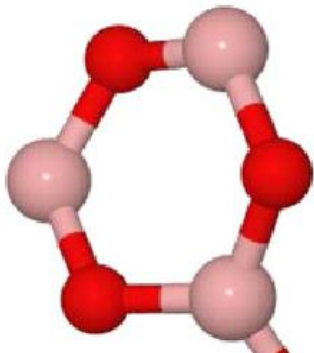
Does liquid or amorphous system diffraction data always support the construction of a completely defined and unique structural model?

The informative case of vitreous B_2O_3

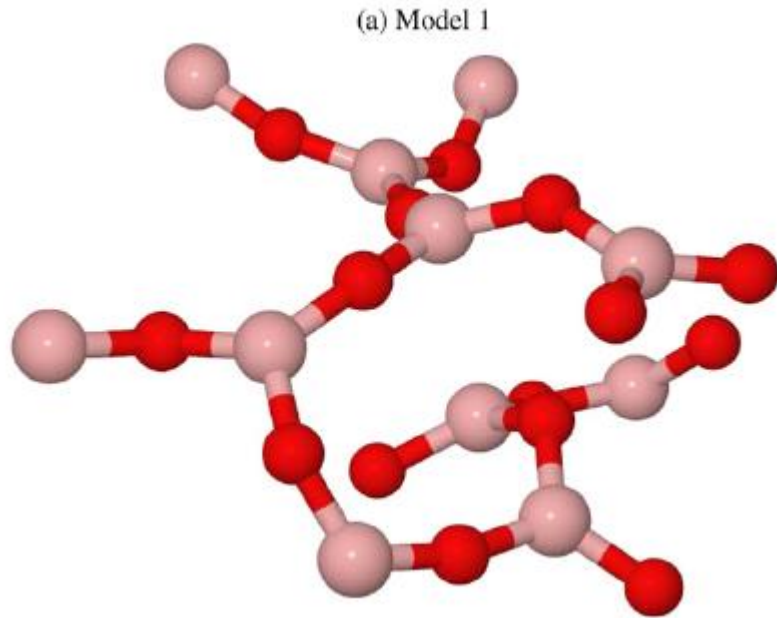
Does vitreous B_2O_3 contain a significant fraction of B_3O_3 ring structures?

Raman scattering and NMR suggest ring fractions of $\approx 70\%$

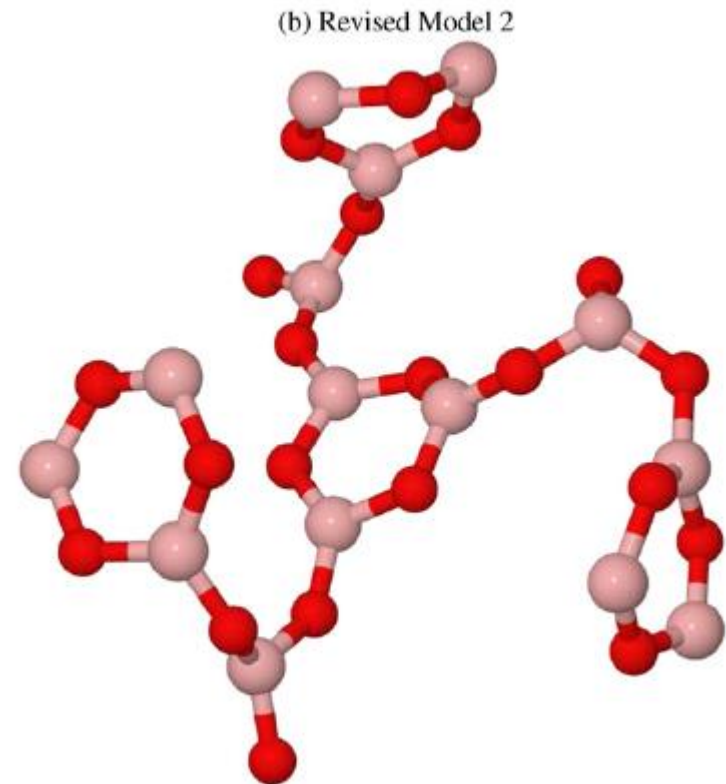
Neutron and X-ray scattering models suggest $< 20\%$



EPSR used as a hypothesis testing framework



6% of boron in boroxyl rings



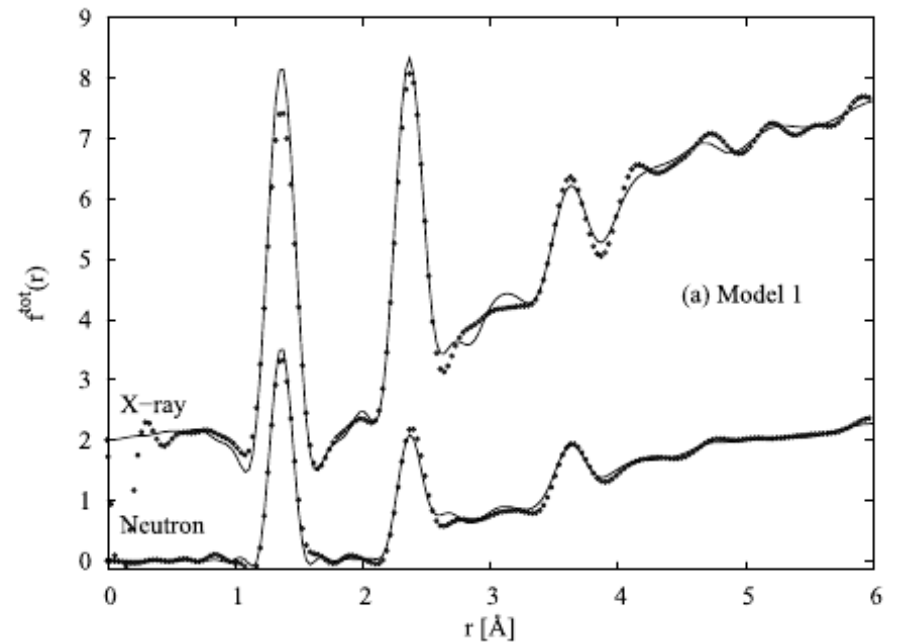
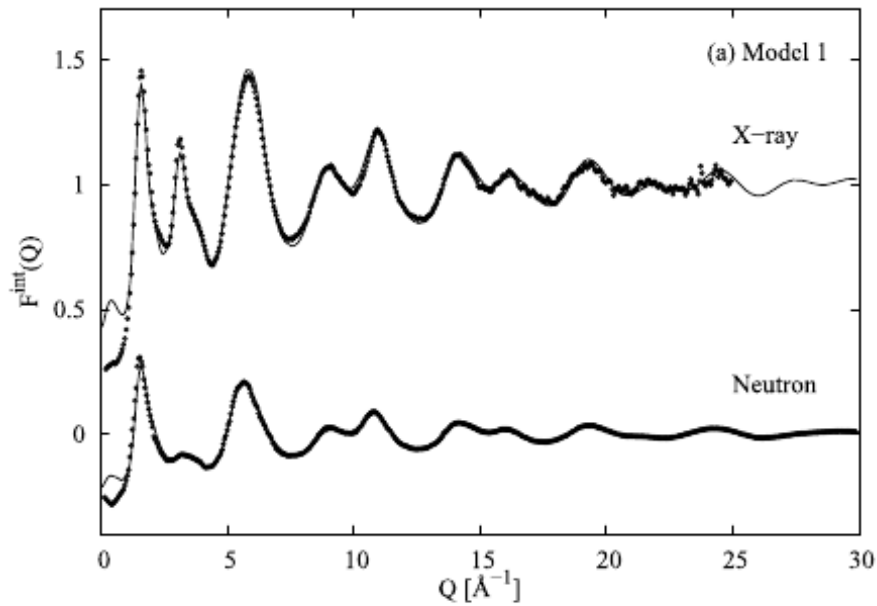
75% of boron in boroxyl rings

EPSR used as a hypothesis testing framework

Model 1: 6% of boron in boroxyl rings

J. Phys.: Condens. Matter **23** (2011) 365402

A K Soper

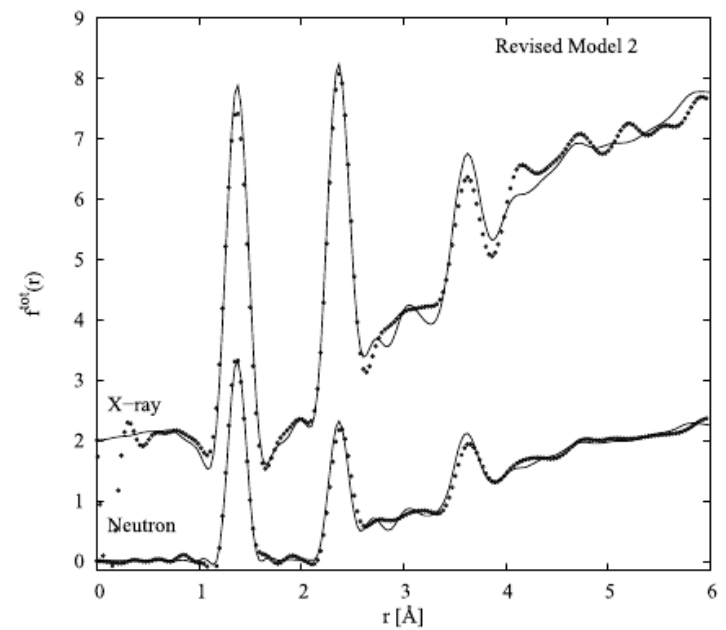
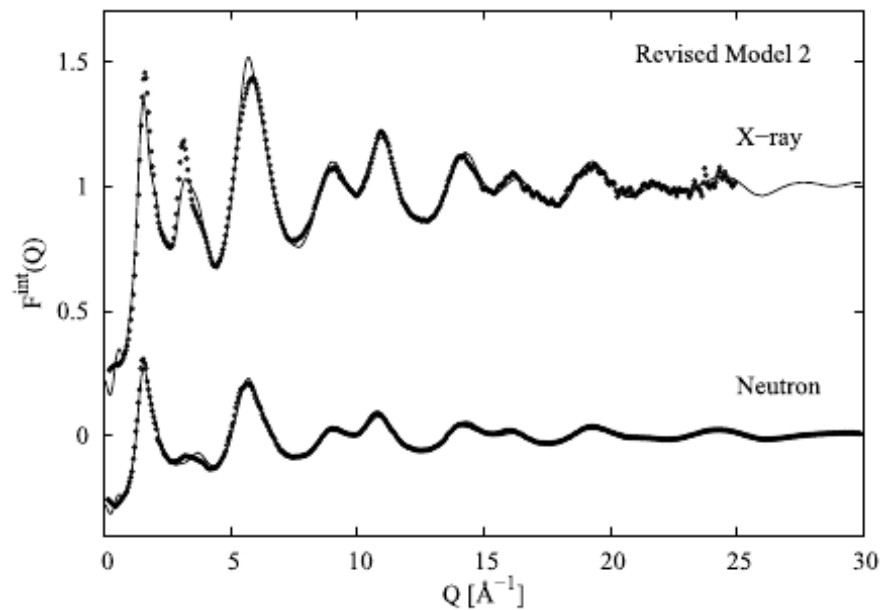


EPSR used as a hypothesis testing framework

Model 1: 75% of boron in boroxyl rings

J. Phys.: Condens. Matter **23** (2011) 365402

A K Soper



EPSR used as a hypothesis testing framework

For the case of vitreous B_2O_3 , the pair correlation sensitivity of diffraction techniques is insufficient to answer the question on ring structures. Such structural motifs not uniquely defined by atomic pair-correlations alone.

EPSR has been used to show that two structurally distinct models are equally capable of reproducing the experimental structure factors.

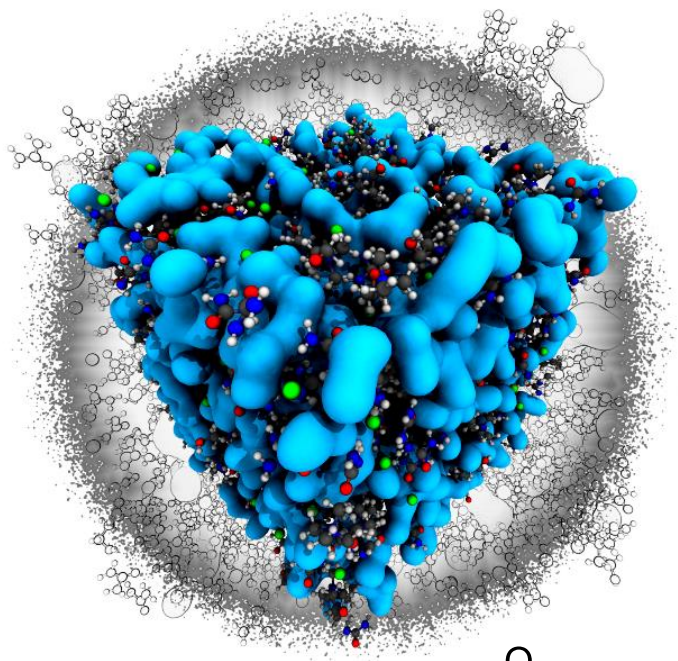
Information from independent experiments is necessary to resolve the issue.

This **uniqueness challenge** is often most acute when attempting to model atomic materials. This is because every building block (atom) is spherical and displays no directional preferences.

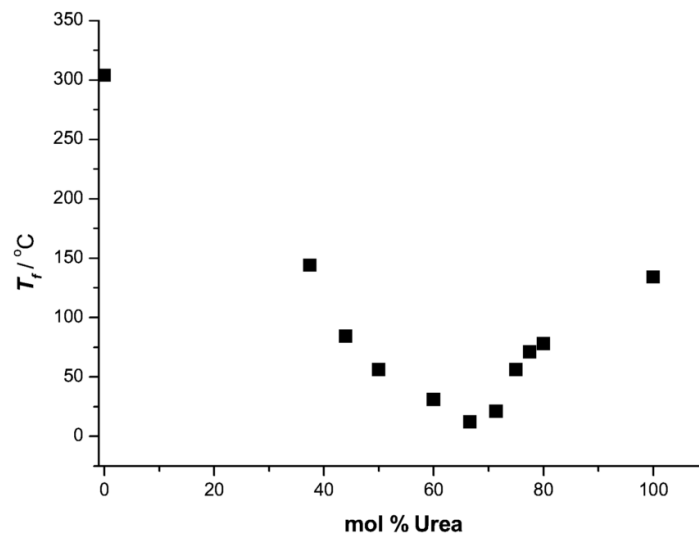
Molecular materials are frequently easier systems to robustly model as the building blocks have distinct shapes and favoured connectivities that place constraints on how the many-body interactions between the atomic sites can be resolved for a given system density.

Recent applications of EPSR

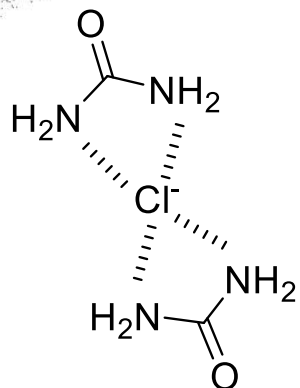
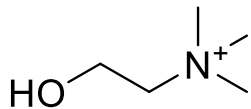
Example 1: The structure of Deep Eutectic Solvents



A salt $[A]^+[B]^-$ mixed with a molecular species $[C]$
Eg: choline chloride-urea (ChCl-Urea)



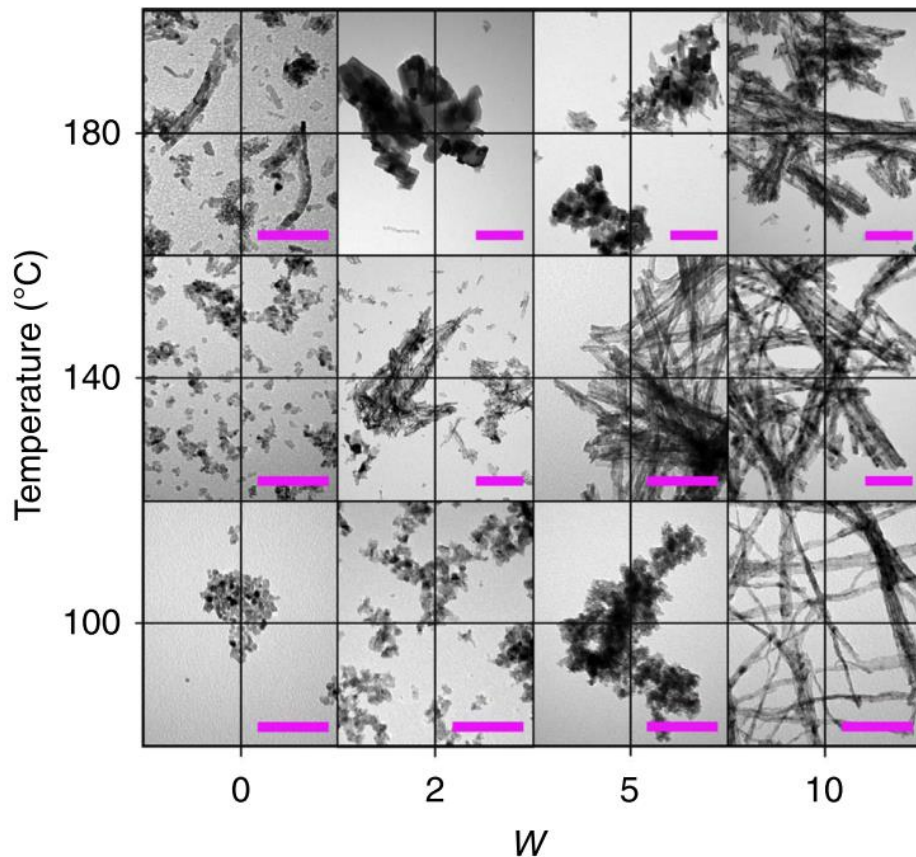
Melting point low at a certain (1:2) mixing ratio



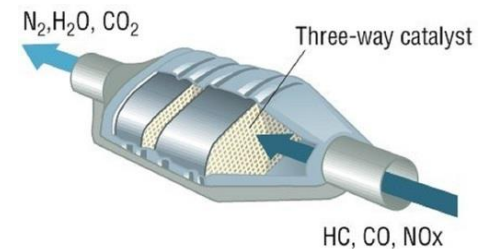
DES can be more environmentally friendly than common ionic liquids (ie. ChCl:U)

DES allow us to design the solvent to be more than a spectator

O.S.Hammond, K.J.Edler, D.T.Bowron and L.Torrente-Murciano, *Nature Comms* (2017) **8** 14150



DES for solvothermal synthesis of nanoparticulate CeO₂



VIP Deep Eutectic Solvents Very Important Paper

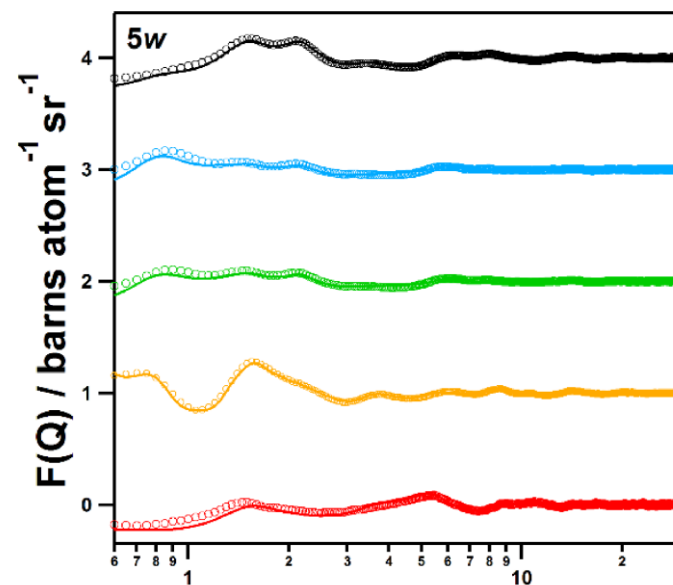
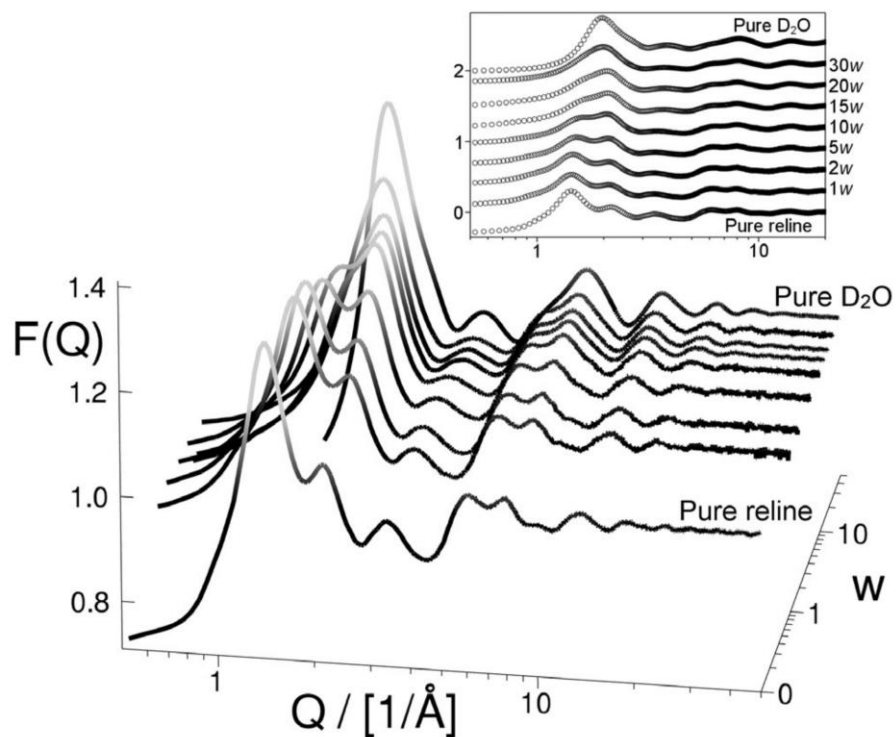
International Edition: DOI: 10.1002/anie.201702486

German Edition: DOI: 10.1002/ange.201702486



The Effect of Water upon Deep Eutectic Solvent Nanostructure: An Unusual Transition from Ionic Mixture to Aqueous Solution

Oliver S. Hammond, Daniel T. Bowron, and Karen J. Edler* *Angew. Chem. Int. Ed.* **2017**, *56*, 9782–9785



VIP **Deep Eutectic Solvents** Very Important Paper

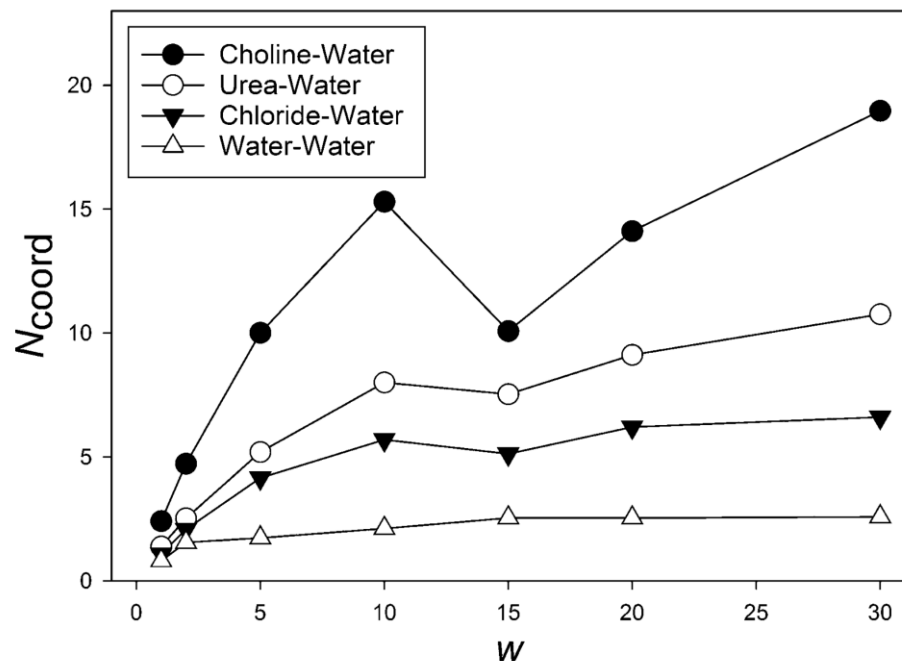
International Edition: DOI: 10.1002/anie.201702486

German Edition: DOI: 10.1002/ange.201702486



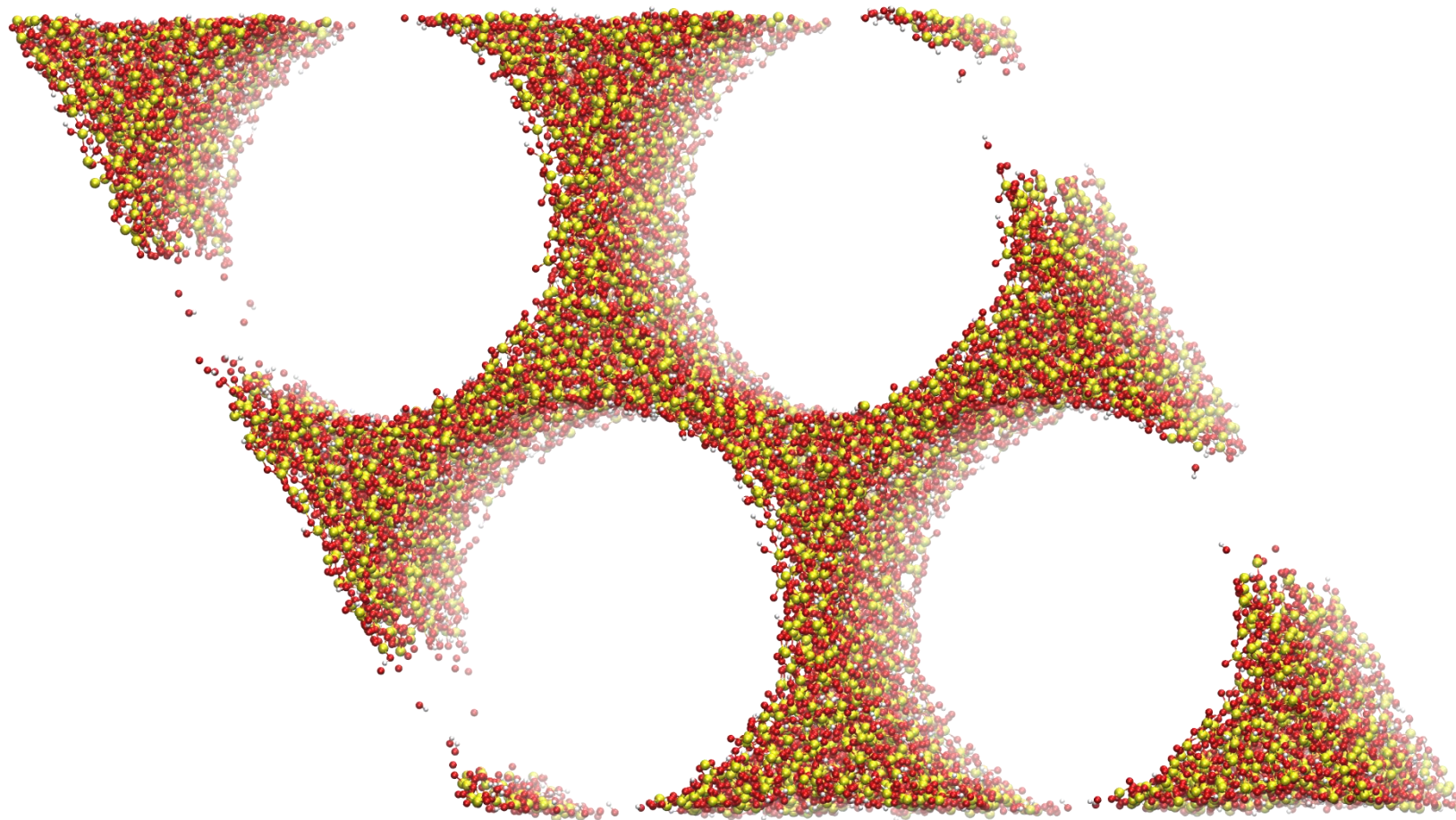
The Effect of Water upon Deep Eutectic Solvent Nanostructure: An Unusual Transition from Ionic Mixture to Aqueous Solution

Oliver S. Hammond, Daniel T. Bowron, and Karen J. Edler* *Angew. Chem. Int. Ed.* **2017**, 56, 9782–9785



At low levels ($\leq 1w$), water contributes slightly to (rather than disrupting) the hydrogen-bonding network, and strengthens choline–urea bonding. This alters the structure enough that it is important for the water content of DES to be characterized. **Between 2w and 10w, the DES–water mixture is in a regime where DES clusters still exist, but are separated by the diluent.** DES intermolecular bonding persists as far as 10w because of the solvophobic sequestration of water into nanostructured domains around choline. **At 15w, we observed a step change in solvation where many of the DES structural motifs cease to be prevalent as water clusters become unfavorable.** At this point, the system is best described as an aqueous solution of DES components at the molecular level.

Example 2a: The structure of MCM-41

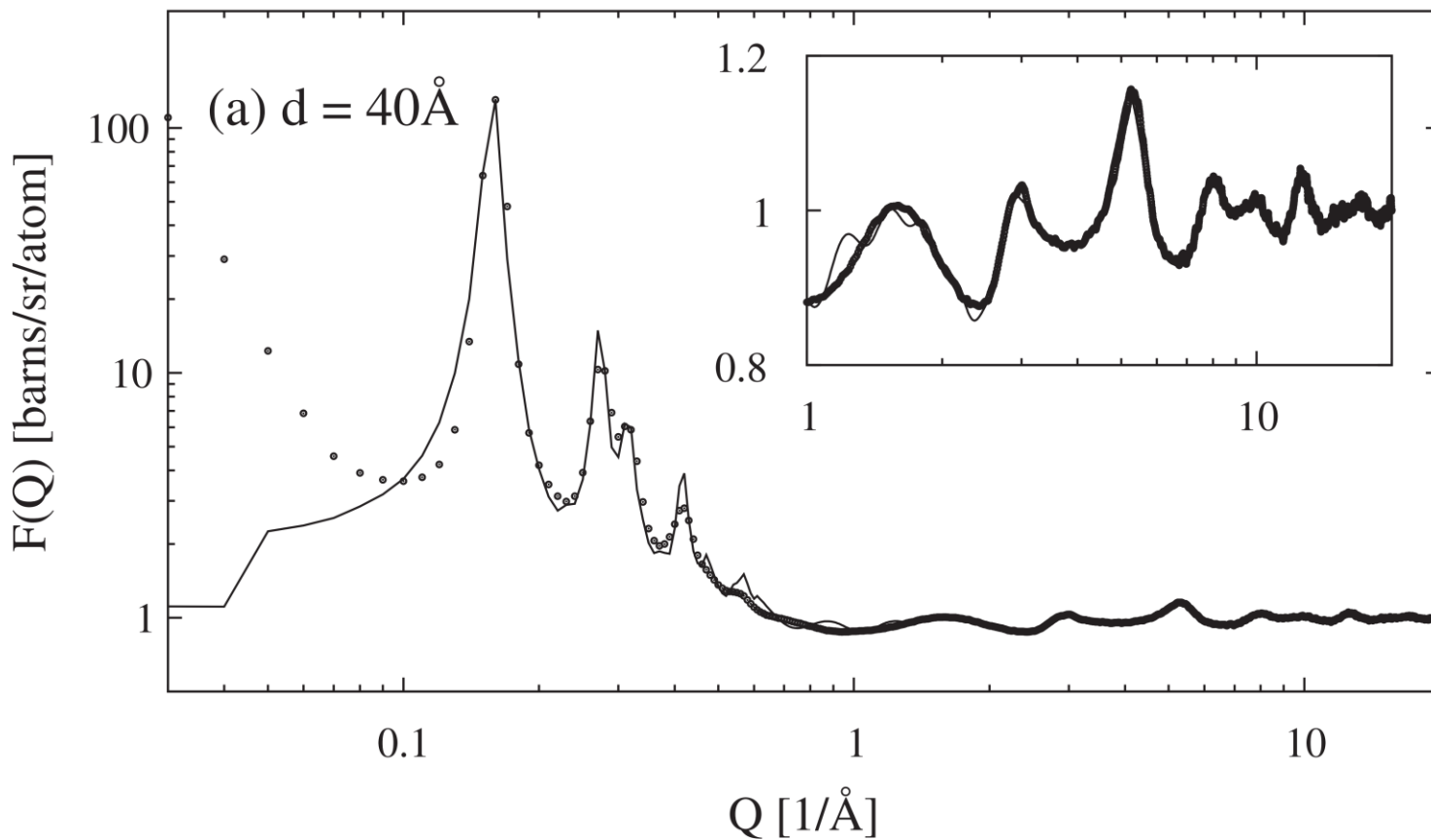


Density profile of nitrogen in cylindrical pores of MCM-41

A.K.Soper and D.T.Bowron

Chem. Phys. Lett. **683** 529-535 (2017)

EPSR refined model of MCM-41

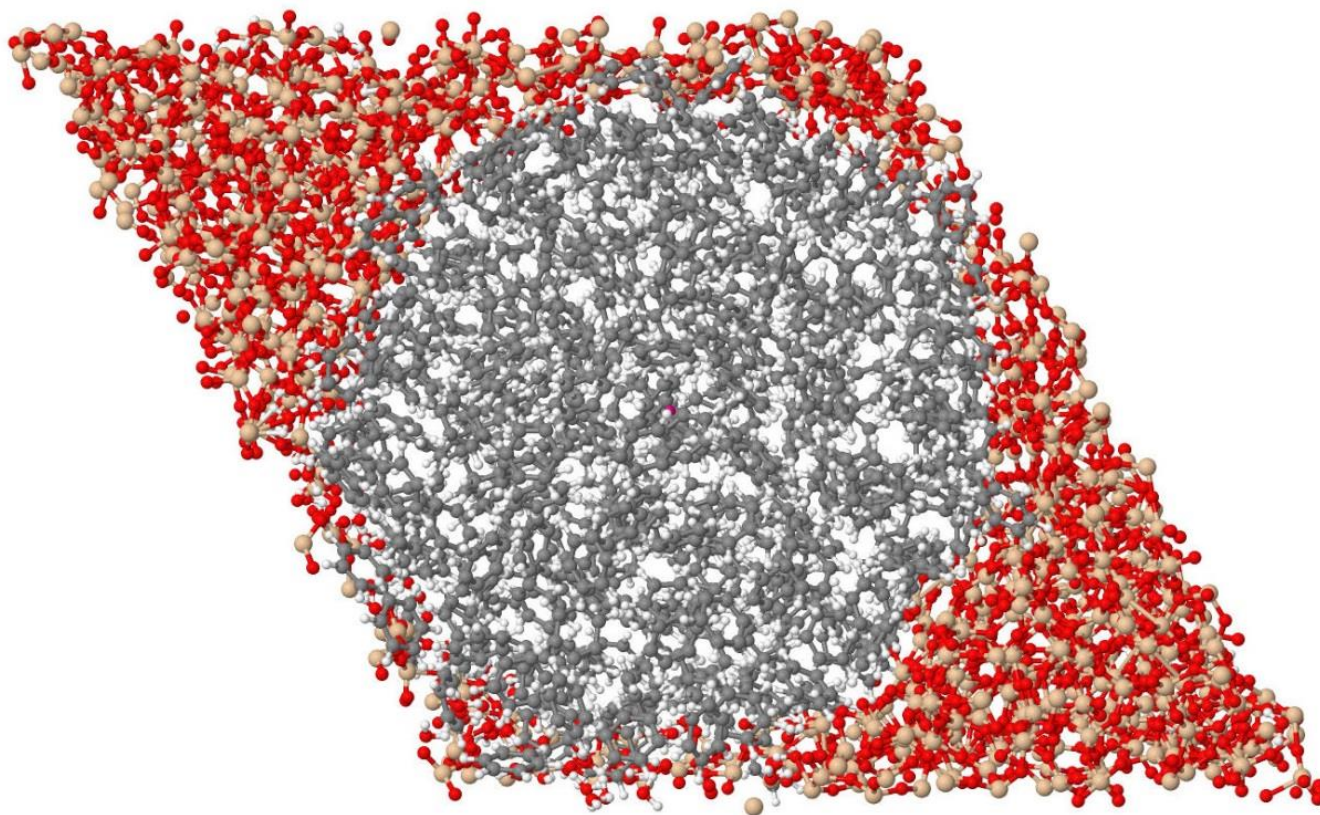


Density profile of nitrogen in cylindrical pores of MCM-41

A.K.Soper and D.T.Bowron

Chem. Phys. Lett. **683** 529-535 (2017)

Example 2b: MCM-41 vapour loaded with liquid benzene



Confinement Effects on the Benzene Orientational Structure

Marta Falkowska, Daniel T. Bowron, Haresh Manyar, Tristan G. A. Youngs

and Christopher Hardacre

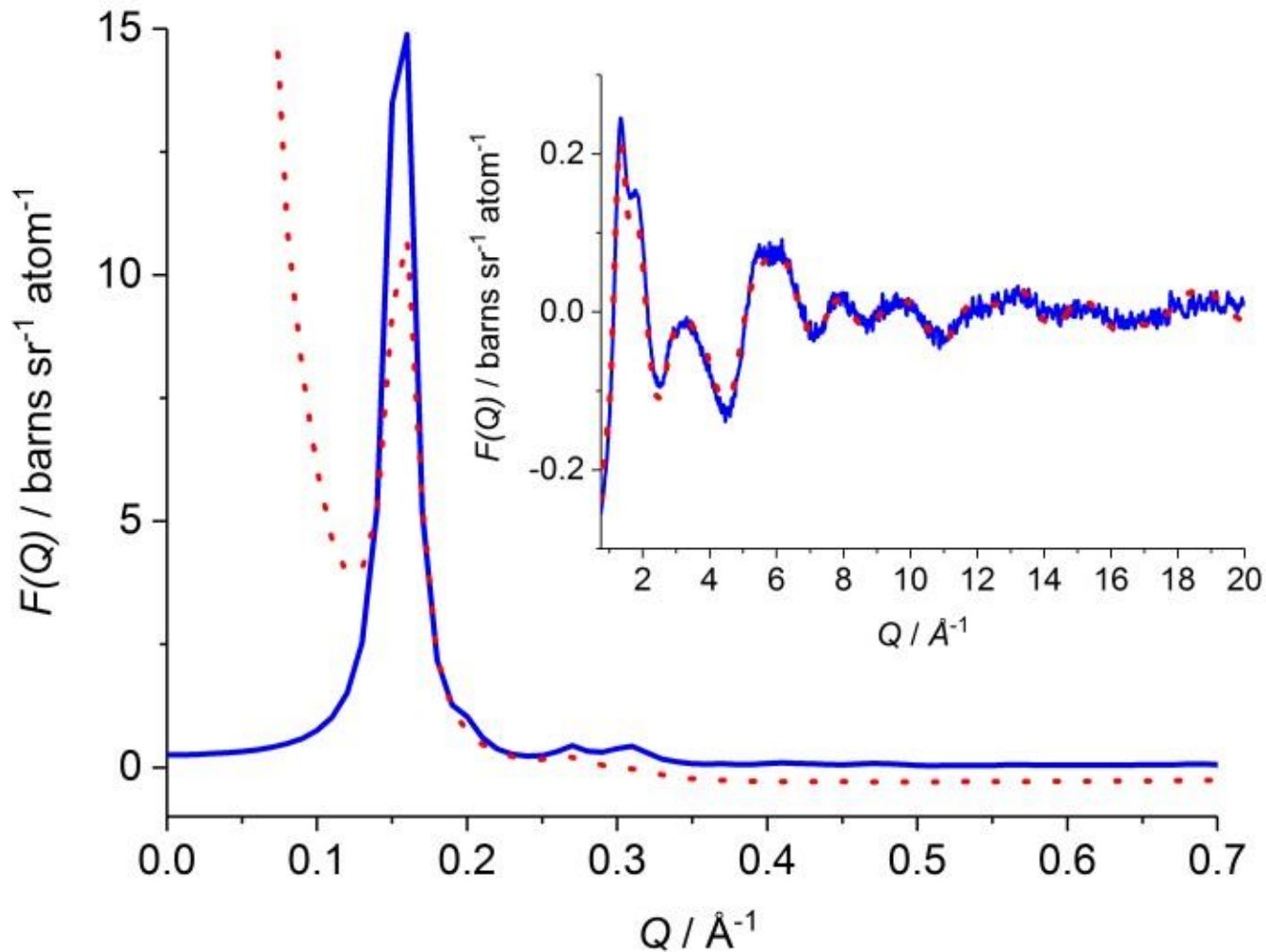
Angew Chemie Intl. Ed. Engl. **57** 4565-4570 (2018)



Science & Technology Facilities Council

ISIS

EPSR model of benzene confined in MCM-41



Confinement Effects on the Benzene Orientational Structure

Marta Falkowska, Daniel T. Bowron, Haresh Manyar, Tristan G. A. Youngs
and Christopher Hardacre

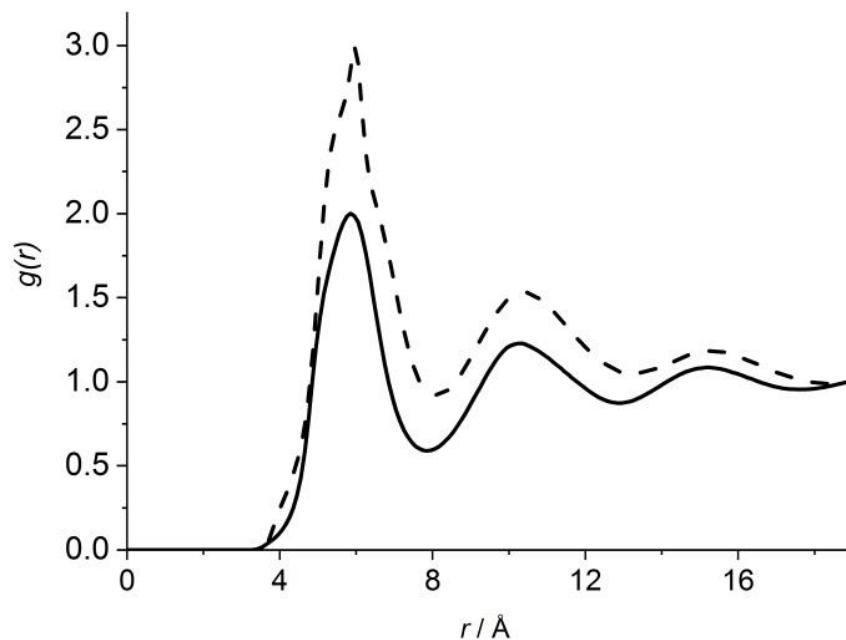
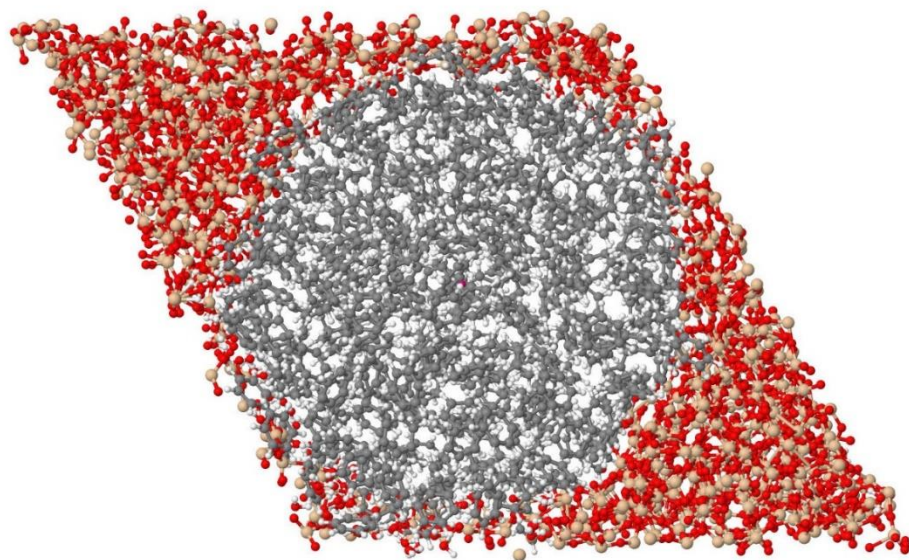
Angew Chemie Intl. Ed. Engl. **57** 4565-4570 (2018)



Science & Technology Facilities Council

ISIS

Radial distribution function of benzene within an MCM-41 pore



Radial distribution functions between molecular centers for benzene- d_6 confined in MCM-41 (dashed line). Solid line represents the radial distribution function for the bulk liquid.

Confinement Effects on the Benzene Orientational Structure

Marta Falkowska, Daniel T. Bowron, Haresh Manyar, Tristan G. A. Youngs

and Christopher Hardacre

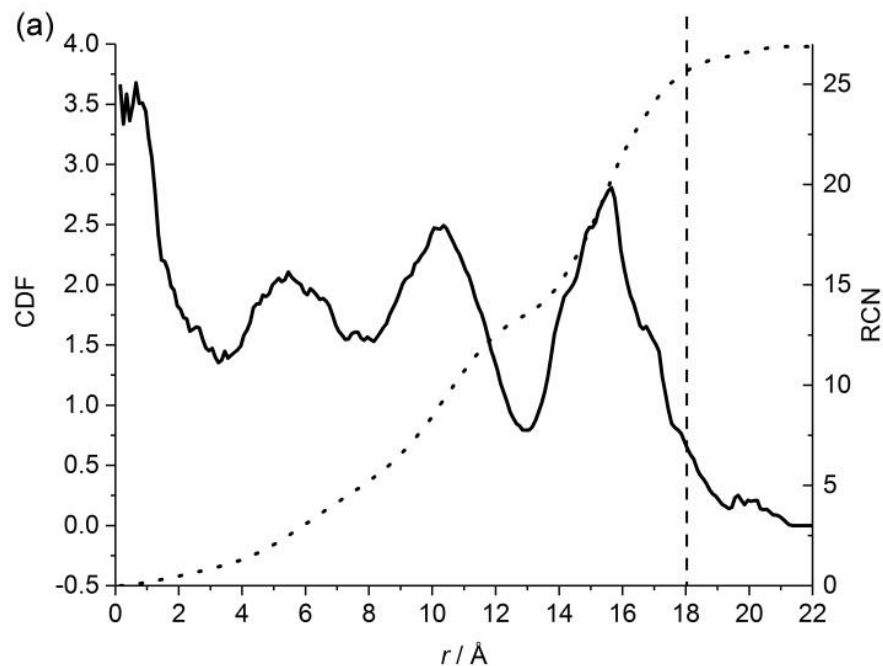
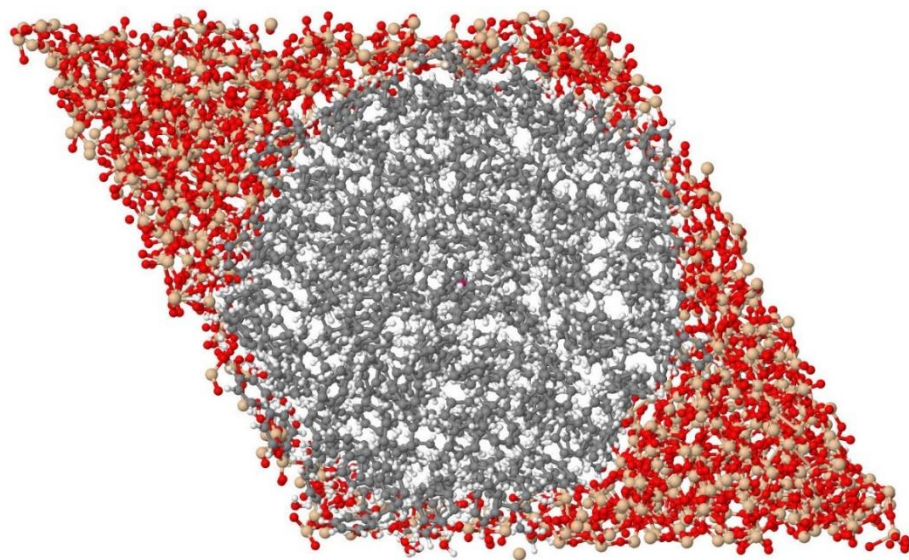
Angew Chemie Intl. Ed. Engl. **57** 4565-4570 (2018)



Science & Technology Facilities Council

ISIS

Cylindrical distribution of benzene within an MCM-41 pore



Cylindrical distribution of benzene centres as a function of pore radius and running coordination number in a 4Å slice along the length of the pore.

Confinement Effects on the Benzene Orientational Structure

Marta Falkowska, Daniel T. Bowron, Haresh Manyar, Tristan G. A. Youngs

and Christopher Hardacre

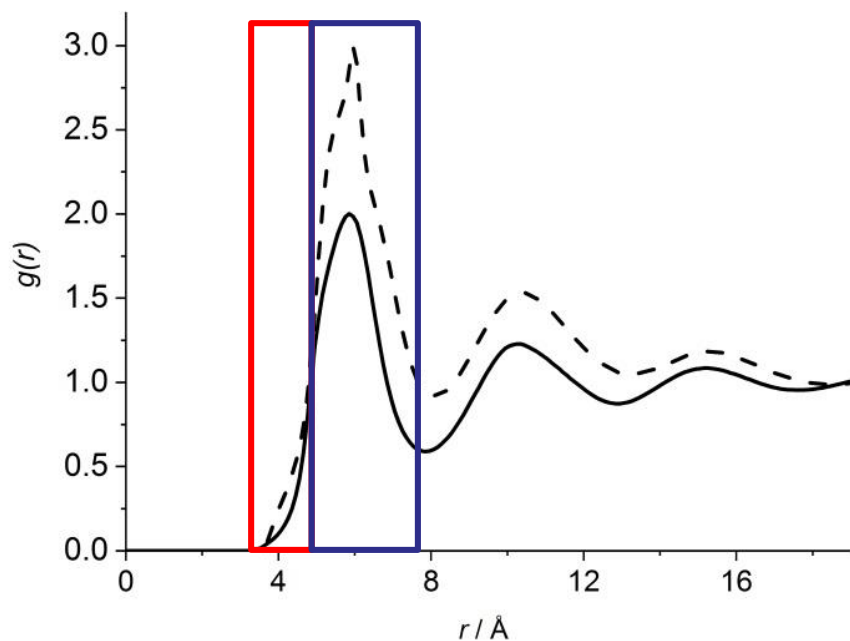
Angew Chemie Intl. Ed. Engl. **57** 4565-4570 (2018)



Science & Technology Facilities Council

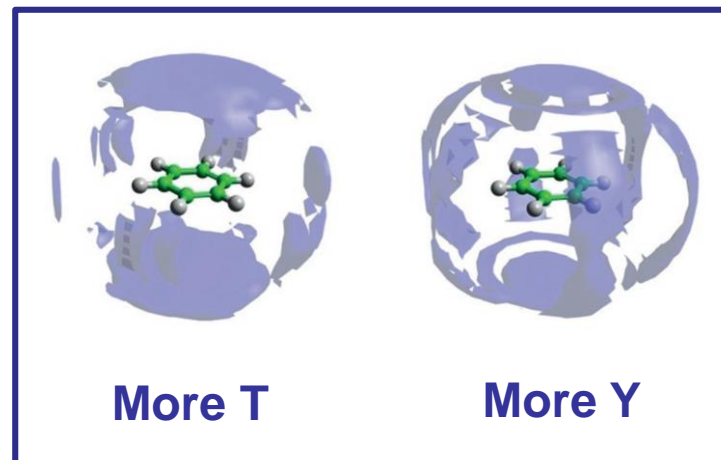
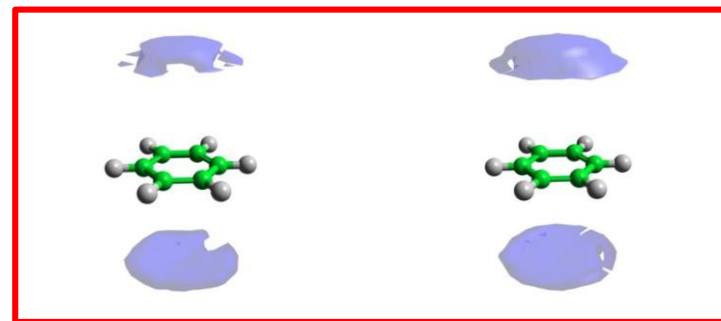
ISIS

Benzene-benzene orientational correlations within an MCM-41 pore



Confined

Bulk



Confinement Effects on the Benzene Orientational Structure

Marta Falkowska, Daniel T. Bowron, Haresh Manyar, Tristan G. A. Youngs

and Christopher Hardacre

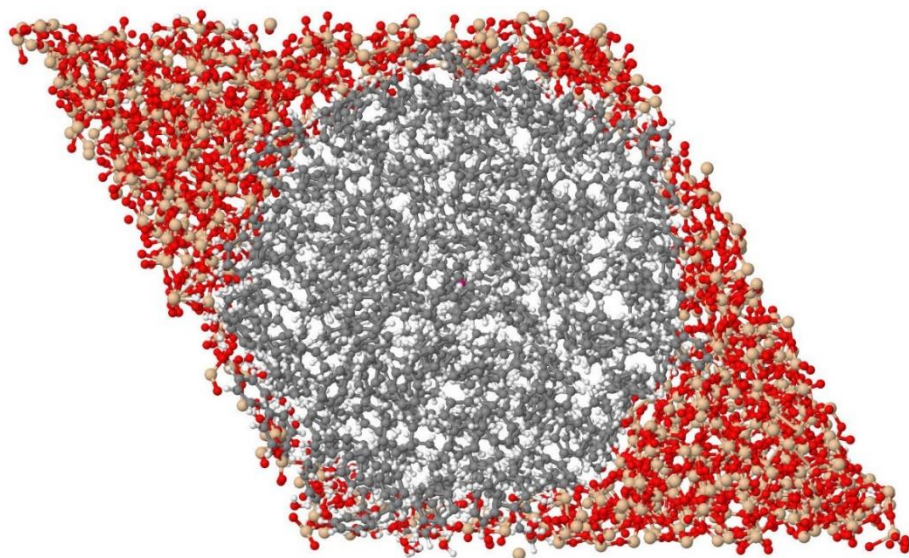
Angew Chemie Intl. Ed. Engl. **57** 4565-4570 (2018)



Science & Technology Facilities Council

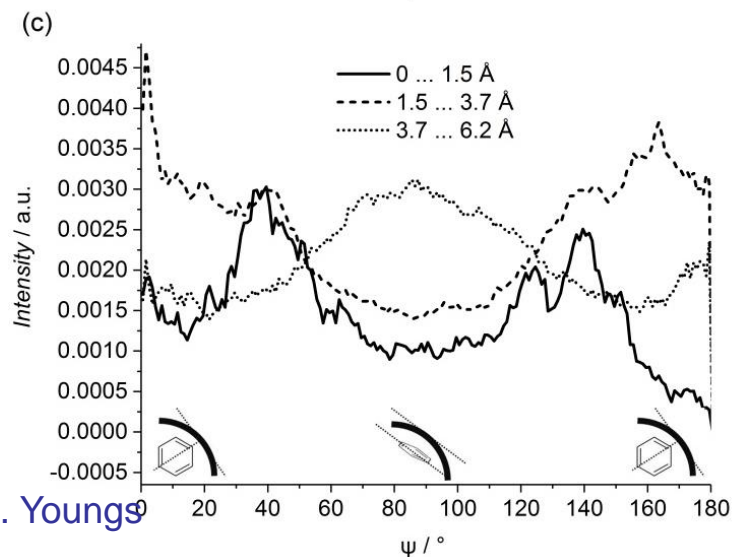
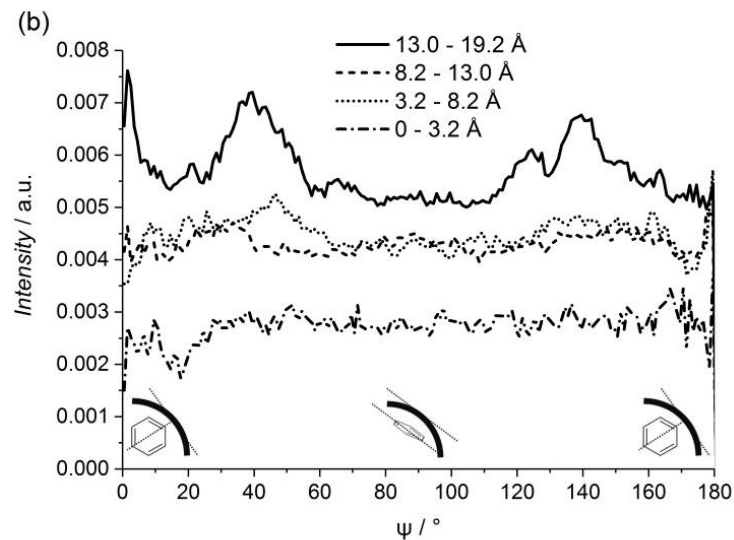
ISIS

Orientational distribution of benzene within an MCM-41 pore



(b) Molecular orientations distribution calculated for each cylindrical concentric shell from centre of the pore.

(c) Molecular orientations distribution calculated for different regions within the concentric cylindrical shell that is located closest to the pore wall.



Confinement Effects on the Benzene Orientational Structure

Marta Falkowska, Daniel T. Bowron, Haresh Manyar, Tristan G. A. Youngs and Christopher Hardacre

Angew Chemie Intl. Ed. Engl. **57** 4565-4570 (2018)



Science & Technology Facilities Council

ISIS

Conclusions: Structure of benzene in MCM-41

- (1) The distribution of molecules across the pore diameter displays well defined layering of the absorbed molecules.
- (2) The confinement of the benzene molecules induces changes in the local ordering when compared with the bulk liquid structure:
 - At short benzene-benzene distances ($<4.85\text{\AA}$) the benzene molecules favour π -stacking
 - At slightly longer distances ($4.85\text{\AA} - 7.90\text{\AA}$) the confined benzene-benzene correlations favour T-configurations (H towards ring centre) over Y-configures found in the bulk (H towards delocalized π -electrons).
- (3) The interaction of benzene molecules with the inner silica-surface of the MCM-41 pore favours a canted configuration with the benzene molecules oriented at an angle of $\sim 40^\circ$ between the ring-plane and the wall surface.

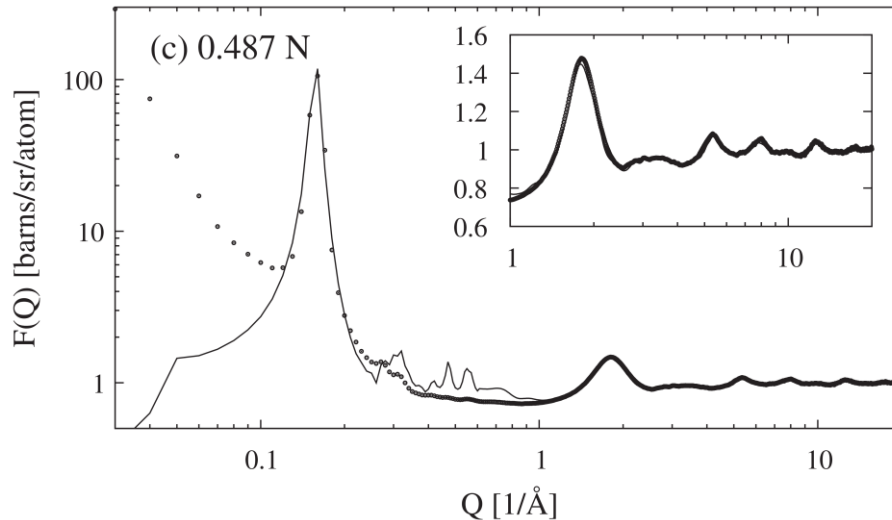
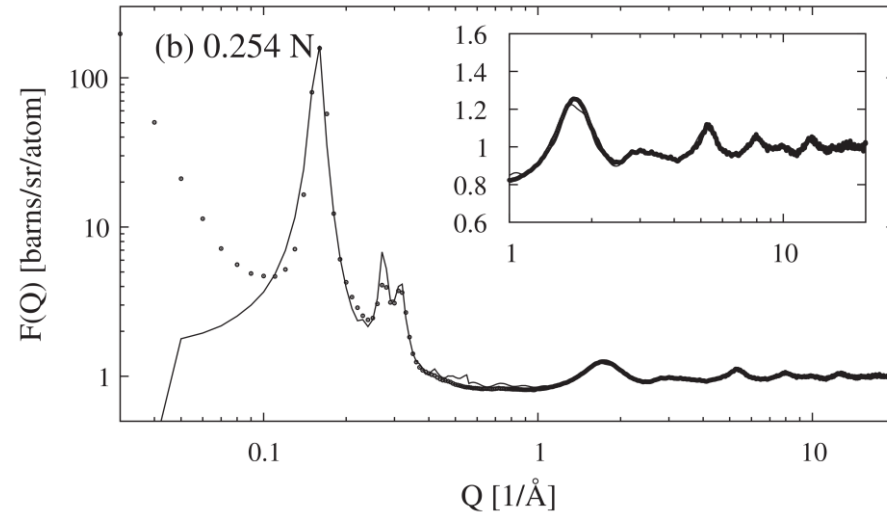
Confinement Effects on the Benzene Orientational Structure

Marta Falkowska, Daniel T. Bowron, Haresh Manyar, Tristan G. A. Youngs

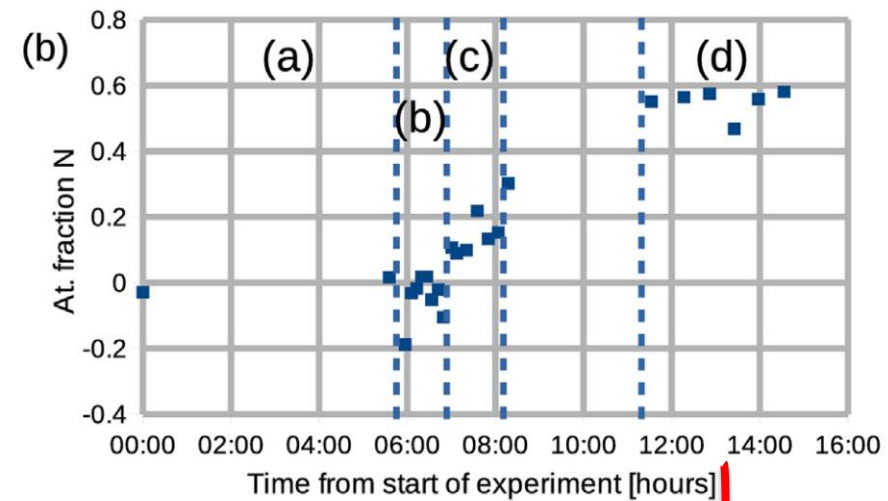
and Christopher Hardacre

Angew Chemie Intl. Ed. Engl. **57** 4565-4570 (2018)

Example 2c: Loading fluids into nanoporous materials: N₂ into MCM-41

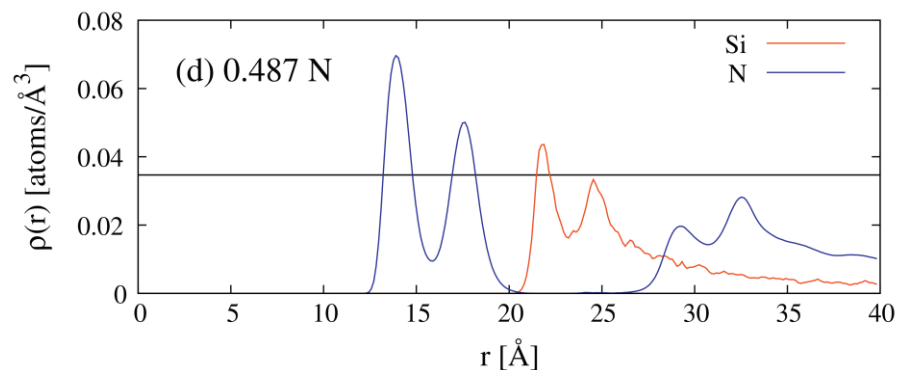
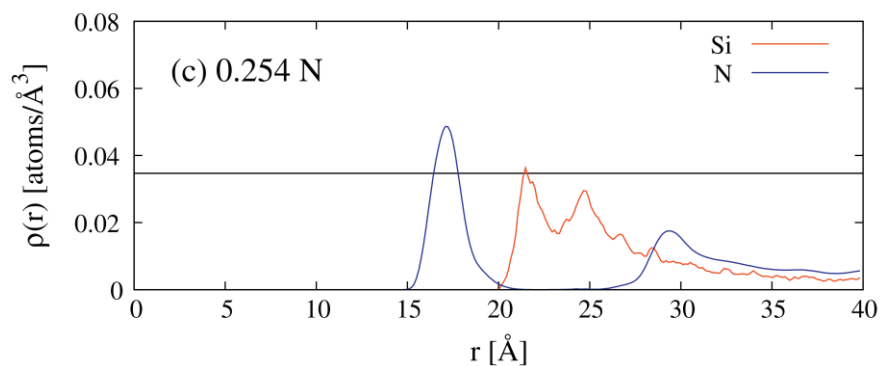
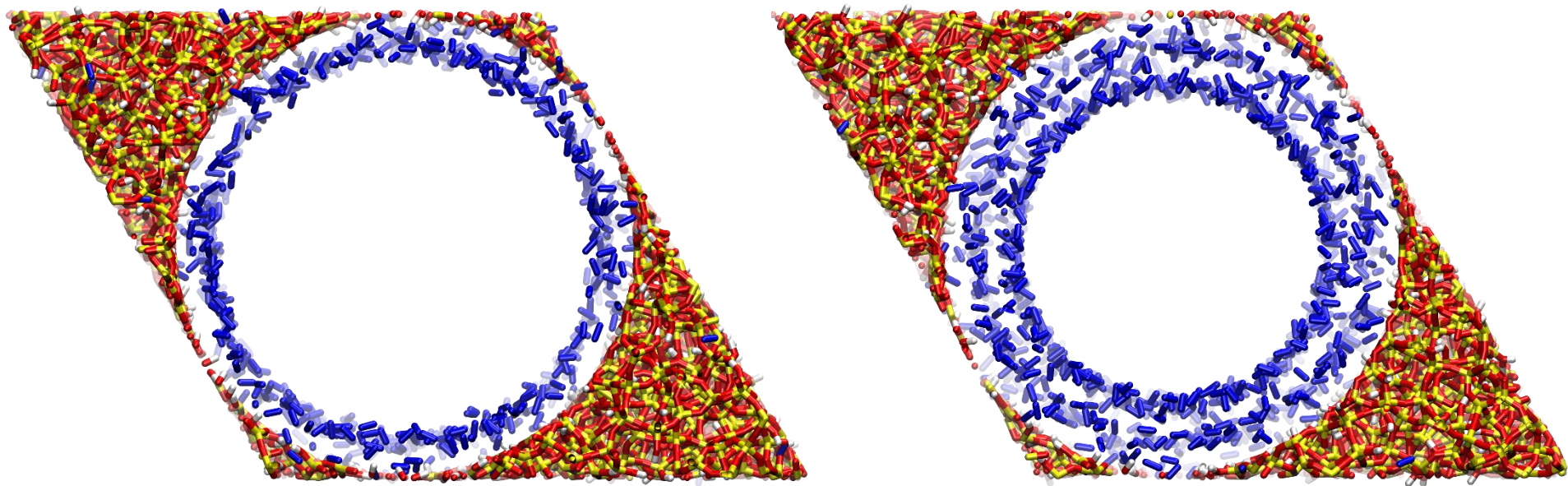


Absorbed N per mole of substrate
 $\text{Si}_{0.28}\text{O}_{0.61}\text{H}_{0.11}$



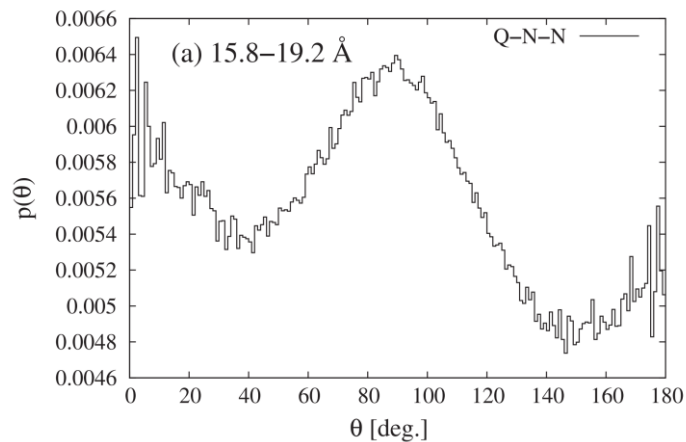
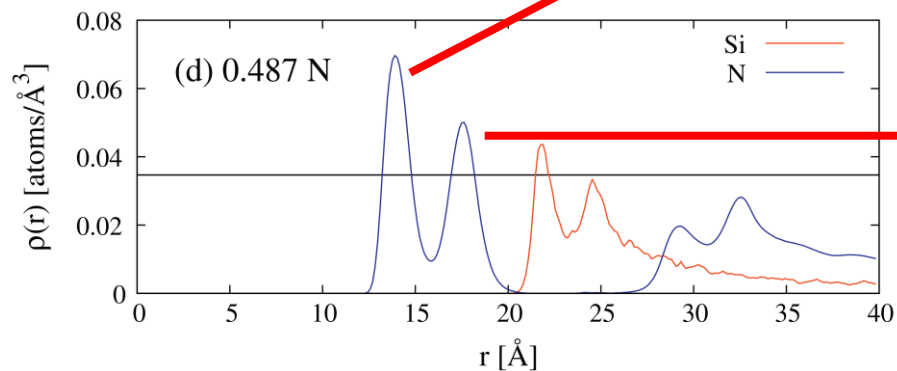
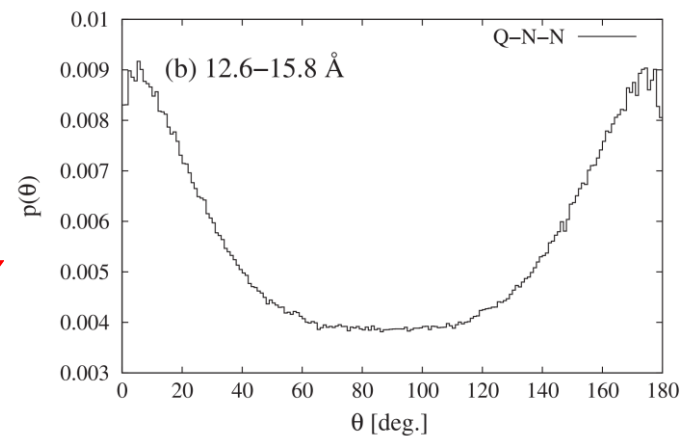
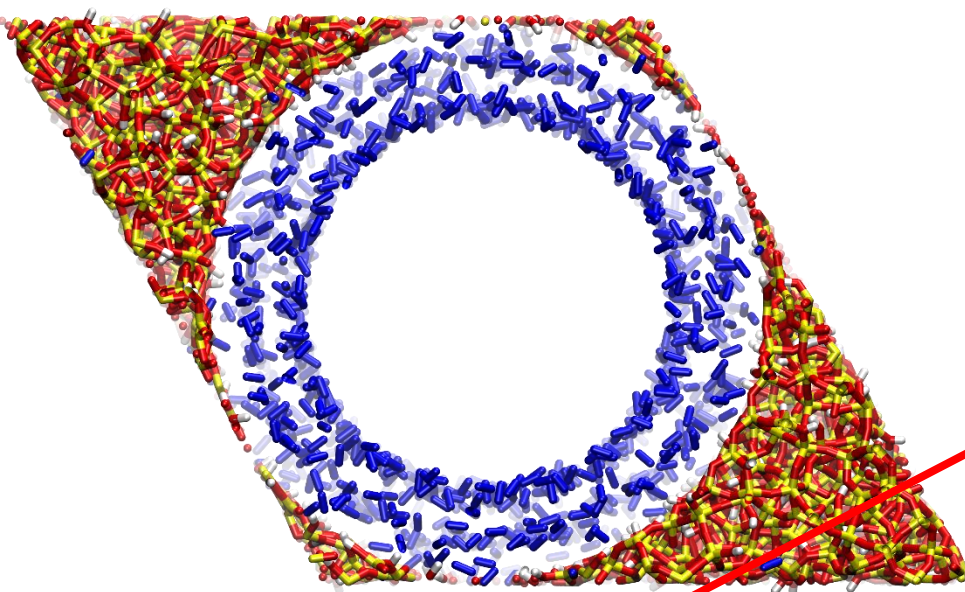
Density profile of nitrogen in cylindrical pores of MCM-41
A.K.Soper and D.T.Bowron
Chem. Phys. Lett. **683** 529-535 (2017)

Example 2c: Loading fluids into nanoporous materials: N₂ into MCM-41



Density profile of nitrogen in cylindrical pores of MCM-41
A.K.Soper and D.T.Bowron
Chem. Phys. Lett. **683** 529-535 (2017)

Orientation of N₂ molecules layered inside MCM-41



Density profile of nitrogen in cylindrical pores of MCM-41
A.K.Soper and D.T.Bowron
Chem. Phys. Lett. **683** 529-535 (2017)

Conclusions: Adsorption of N₂ in MCM-41

- (1) Before the onset of capillary condensation of nitrogen into MCM-41 the gas is strongly adsorbed in distinct layers inside the pore space.
- (2) Each layer of nitrogen has a strong orientational configuration
 - The layer of N₂ molecules closest to the silica surface prefers to lie flat with the long-axis of the molecule parallel with the surface.
 - The second layer of N₂ molecules favours a configuration where the long-axis of the molecule is oriented radially with respect to the pore axis.

Density profile of nitrogen in cylindrical pores of MCM-41

A.K.Soper and D.T.Bowron

Chem. Phys. Lett. **683** 529-535 (2017)

Empirical Potential Structure Refinement

Summary of Current Status

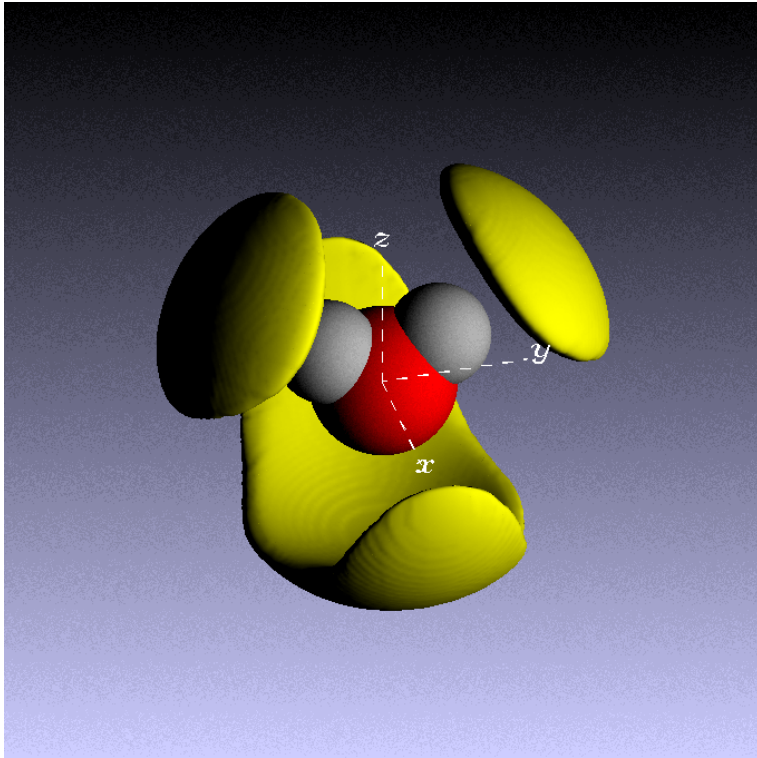
EPSR version 25

Atomic and molecular liquids	Yes
Atomic and molecular glasses	Yes
Neutron scattering data	Refine
X-ray scattering data	Refine
Large scale systems	100Å (120Å at a push) 150000 atoms 50000 molecules
Mesostructured systems	Yes
Ordered and partially ordered systems	Yes
Bragg scattering modeling	Yes
GUI front end	Yes

Empirical Potential Structure Refinement

Download your copy of EPSR from:

<https://www.isis.stfc.ac.uk/Pages/Empirical-Potential-Structure-Refinement.aspx>



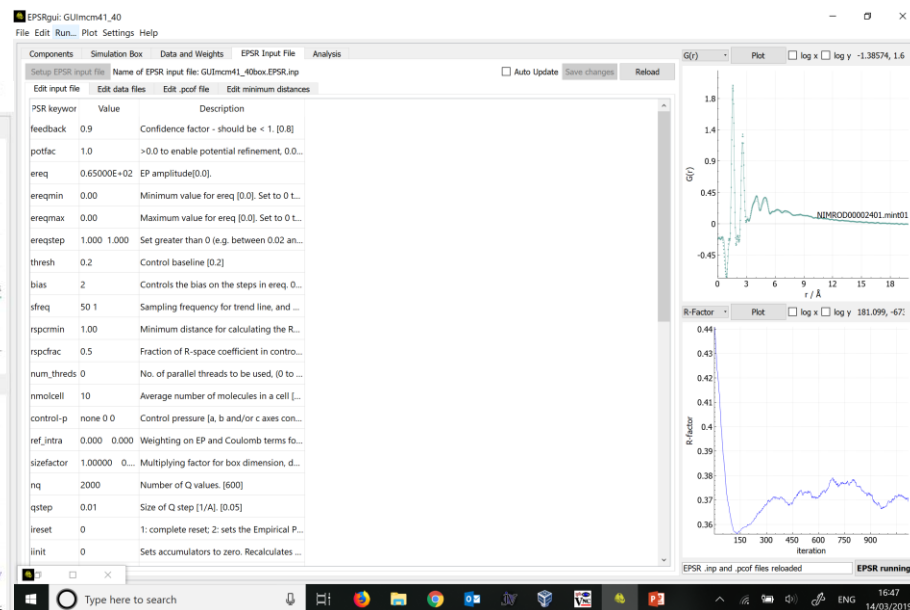
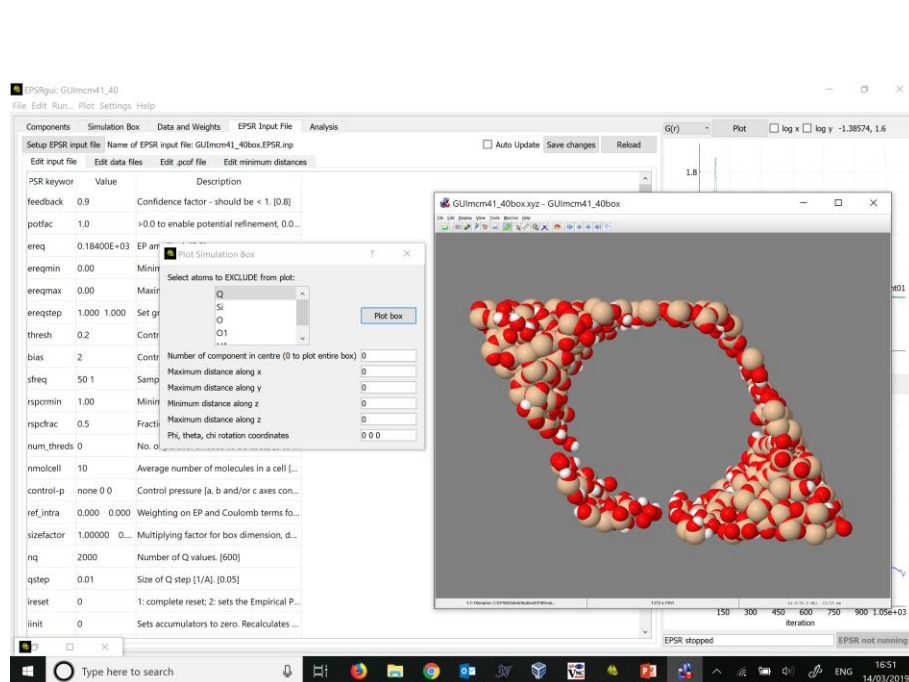
$$U_{\alpha\beta}^N = U_{\alpha\beta}^O(\mathbf{r}) + U_{\alpha\beta}^{\Delta EP}(\mathbf{r})$$

A.K.Soper *Chem Phys* **202** p.295 (1996)
A.K.Soper *Phys Rev B* **72** 104204 (2005)

EPSRgui: A more intuitive way to run EPSR

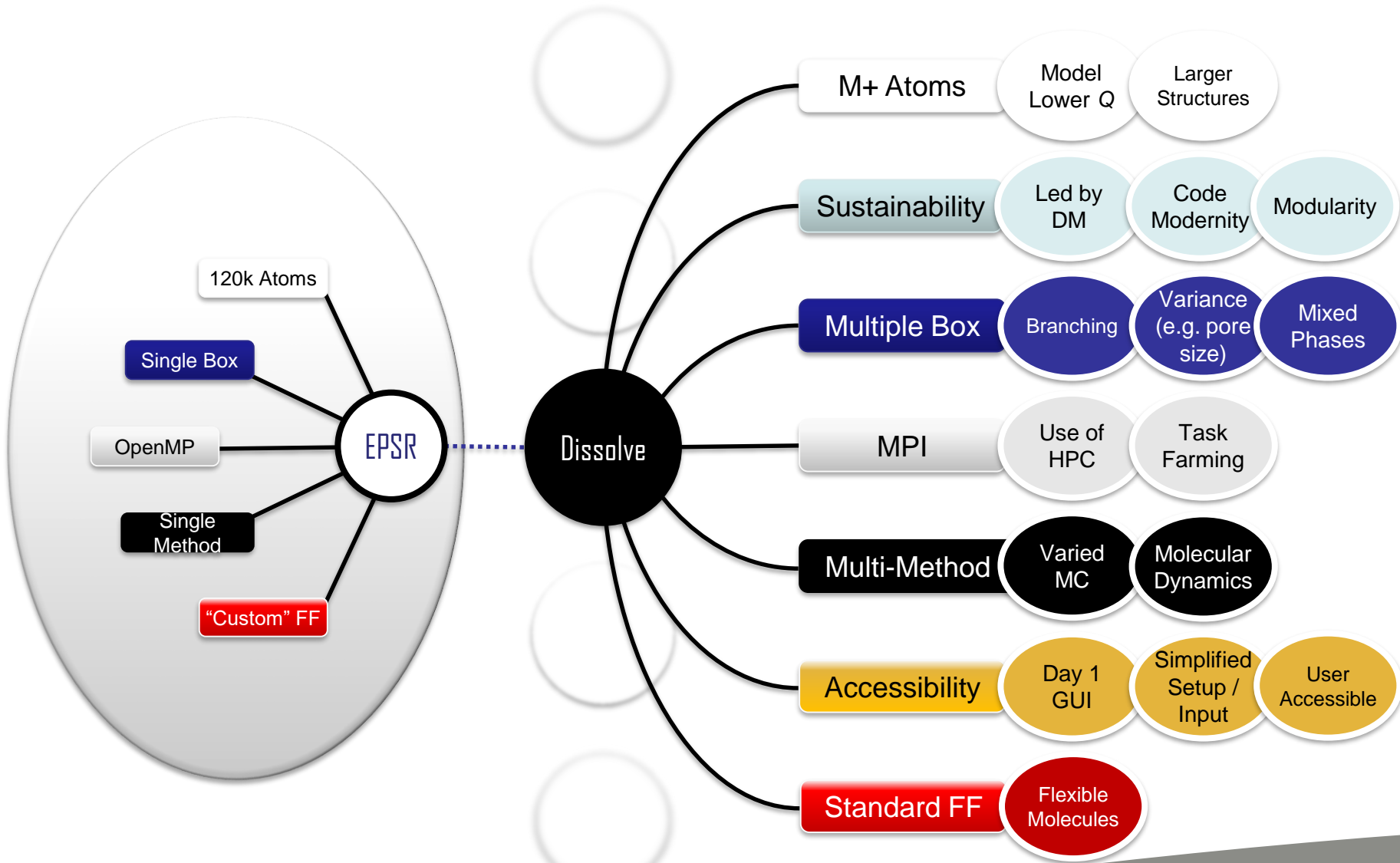
Download your copy of EPSRgui from:

<https://www.isis.stfc.ac.uk/Pages/Empirical-Potential-Structure-Refinement.aspx>



S.K.Callear, Rutherford Appleton Laboratory Technical Report
RAL-TR-2017-002

The future of EPSR - dissolve

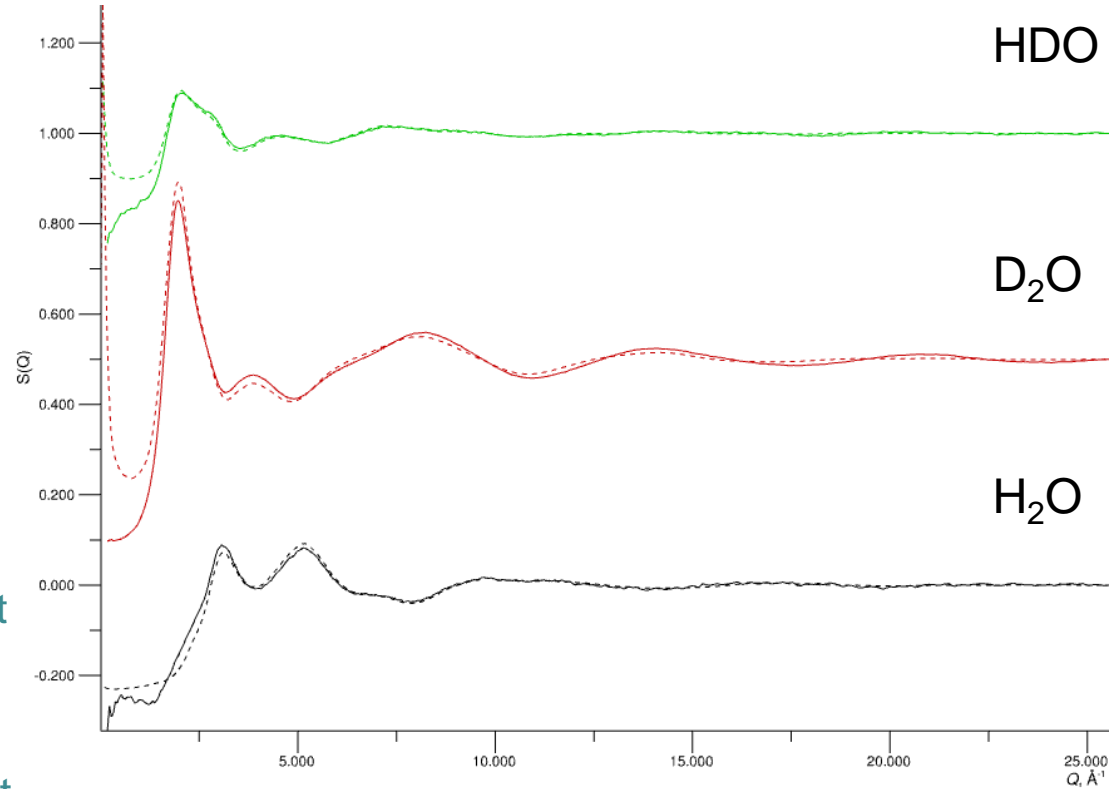


<https://github.com/trisyongs/dissolve>

Dissolve – current status

- ✓ Monte Carlo
- ✓ Molecular dynamics
- ✓ Full user interface
- ✓ Potential refinement
- ✓ Million atom capable
 - 333,334 SPC/FW water
 - 15 Å cutoff
 - RDF $r_{max} = 107.7$ Å
 - 4 days / 8 cores on SCARF

- Molecule MC : 2 m 40 s / it
- Intra MC : 4 m 30 s / it
- Partial $g(r)$: 29 m 30 s / it
- Energy : 20 s / it



<https://github.com/trisyongs/dissolve>